



Estimation of Submarine Near-Bottom Hydrodynamic Loads and Squat

M. Mackay

Defence R&D Canada

Technical Memorandum

DRDC Atlantic TM 2003-078

April 2003

Copy No. _____

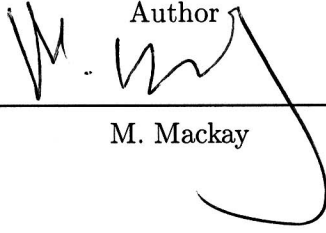
Estimation of Submarine Near-Bottom Hydrodynamic Loads and Squat

M. Mackay

Defence R&D Canada – Atlantic

Technical Memorandum
DRDC Atlantic TM 2003-078
April 2003

Author



M. Mackay

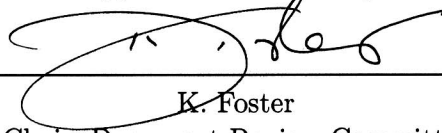
Approved by



N. Pegg

Head, Warship Performance

Approved for release by



K. Foster

Chair, Document Review Committee

Abstract

This memorandum outlines a method for estimating the near-bottom loads on a submarine submerged in deep water and for the related problem of predicting submarine squat in deep or shallow water. The method is fully three-dimensional, but has some limitations associated with potential flow and linearization of the free surface. The chief difficulty for this study was the dearth of suitable data available for validation. Nevertheless, the results are encouraging. Overall, it appears that the sinkage component of squat is predicted with greater accuracy than is trim. Further work should include the acquisition of more, reliable, model data and the investigation of scale effects.

Résumé

Le présent document donne un bref aperçu d'une méthode d'estimation des charges près du fond d'un sous-marin en plongée en eaux profondes et des problèmes connexes de prédiction de l'accroupissement d'un sous-marin en eaux profondes ou peu profondes. La méthode est entièrement tridimensionnelle, mais comporte certaines limites relatives à l'écoulement potentiel et à la linéarisation de la surface libre. Malgré la rareté des données appropriées disponibles pour validation, principale difficulté rencontrée lors de l'étude, les résultats sont encourageants. Dans l'ensemble, le composant enfoncement de l'accroupissement semble être plus facile à prédire que l'assiette. Les travaux à venir devraient comprendre l'acquisition de plus de données de modélisation fiables et l'analyse des effets de changement d'échelle.

This page intentionally left blank.

Executive Summary

Introduction

Prompted by interest in the hazards associated with submarine operation in confined water, an exploratory study was made of a potential flow-based method of predicting near-bottom loads and squat. This memorandum outlines the method and some validation with experimental data.

Significance

A submarine operating near the sea bottom experiences a downforce and pitching moment that complicates maintaining bottom clearance. Squat, the increase in draft when underway on the surface, is increased by these loads when in shallow water. Understanding and predicting these effects is important to the safe operation of the Victoria class.

Principal Results

The estimation method described here predicts near-bottom loads and squat reasonably well compared with the few suitable validation data that were found. However, the trim component of squat appears to be difficult for this and other methods to predict with accuracy, and furthermore is not easy to measure. More, reliable, experimental data are needed. The effects of scaling model experiments to full scale should be investigated further.

Further Investigations

It is planned to do near-bottom experiments with a model of the Victoria class in 2003.

M. Mackay, 2003, Estimation of Submarine Near-Bottom Hydrodynamic Loads and Squat, DRDC Atlantic TM 2003-078.

Defence R&D Canada – Atlantic.

Sommaire

Introduction

Étant donné l'intérêt porté aux risques rattachés aux déplacements des sous-marins en eaux restreintes, une étude préliminaire portant sur une méthode de prédiction, basée sur l'écoulement, des charges près du fond et de l'accroupissement a été menée. Le présent document donne un aperçu de la méthode et de la validation obtenue à l'aide de données expérimentales.

Importance

Un sous-marin qui se déplace près du fond de la mer est soumis à une portance négative et à un moment de tangage qui nuisent au maintien du dégagement sous la coque. En eaux peu profondes, ces forces augmentent l'accroupissement, qui équivaut, en surface, à l'augmentation du tirant d'eau lors du déplacement. Il est important de comprendre et de prédire l'effet de ces forces pour assurer la sécurité de fonctionnement des sous-marins de classe Victoria.

Principaux résultats

La méthode d'estimation décrite dans le présent document permet de prédire assez bien les charges près du fond et l'accroupissement, si l'on se fie aux quelques données de validation pertinentes disponibles. Cependant, l'élément d'assiette de l'accroupissement semble difficile à prédire avec précision, autant selon cette méthode que selon d'autres, et est difficile à mesurer. Il faudrait plus de données expérimentales fiables. Une analyse plus poussée des effets de changement d'échelle, essais sur maquettes à essais en vraie grandeur, doit être faite.

Travaux futurs

Des expériences sur les charges près du fond devraient être effectuées en 2003 avec un modèle de sous-marin de classe Victoria.

M. Mackay, 2003, Estimation of Submarine Near-Bottom Hydrodynamic Loads and Squat, DRDC Atlantic TM 2003-078.

R & D pour la défense Canada – Atlantique.

Table of Contents

Abstract	i
Résumé	i
Executive Summary	iii
Sommaire	iv
Table of Contents	v
List of Figures	vi
1 Introduction	1
2 Calculation Methods	2
2.1 Potential Flow	2
2.2 Hydrostatics	3
3 Comparison of Near-Bottom Loads	3
3.1 Sphere Moving Parallel to a Boundary	4
3.2 Submarine Model Experiments	5
4 Comparison of Squat Results	6
4.1 CPF in Deep and Shallow Water	6
4.2 Submarine in Shallow Water	8
5 Concluding Remarks	10
References	11
Annex A. Hydrostatic Calculation Worksheet for Surface Ship	28
Annex B. Hydrostatic Calculation Worksheet for Submarine	34
Nomenclature	39

List of Figures

Figure 1.	Equivalence of potential flow and the discrete model	13
Figure 2.	PC967 geometry setup for three configurations	13
Figure 3.	Sphere paneling	14
Figure 4.	Axial pressure distribution on an isolated sphere	14
Figure 5.	Force coefficient on a sphere moving parallel to a plane	15
Figure 6.	Pressure coefficient round the near-midsection of a sphere moving parallel to a plane	15
Figure 7.	Stretched spheres	16
Figure 8.	Axial pressure distribution on isolated stretched spheres	16
Figure 9.	Force coefficient on a sphere and stretched sphere moving parallel to a plane	17
Figure 10.	Representative hull for comparison with near-bottom model experiments	17
Figure 11.	Submarine near bottom: downforce plotted against $2r/c$	18
Figure 12.	Submarine near bottom: pitching moment plotted against $2r/c$..	18
Figure 13.	Submarine near bottom: downforce plotted against h/r	19
Figure 14.	Submarine near bottom: pitching moment plotted against h/r ..	19
Figure 15.	Paneling for the CPF hull and its image	20
Figure 16.	CPF deep water squat	20
Figure 17.	CPF: longitudinal distribution of downforce calculated by PC967	21
Figure 18.	Nondimensional CPF beam and area	21
Figure 19.	CPF: shallow water AP squat estimates	22
Figure 20.	CPF: shallow water FP squat estimates	22
Figure 21.	Actual geometry for a surfaced submarine hull, and PC967 approximations for deep and shallow water	23
Figure 22.	Submarine hull paneling for comparison with squat experiments	23
Figure 23.	Longitudinal distribution of downforce estimated by PC967 for SSBN05 hull with and without a keel	24
Figure 24.	Submarine squat: sinkage data for SSBN05	24
Figure 25.	Nondimensional SSBN05 beam and area	25
Figure 26.	Submarine squat: comparison of SSBN05 model data with the Vermeer and Millward methods.....	25
Figure 27.	Estimated nondimensional boundary layer displacement thickness for SSBN05 hull	26
Figure 28.	Submarine squat: comparison of SSBN05 model data with the present method	26
Figure 29.	Submarine squat: predicted sinkage at LCF for SSBN05	27
Figure 30.	Submarine squat: predicted trim for SSBN05	27

1 Introduction

This memorandum discusses a method for estimating near-bottom hydrodynamic loads on a submarine submerged in deep water and for the related problem of predicting squat for a submarine on the surface in deep or shallow water. The investigation was first prompted by concerns for confined water operation of the CF Victoria class. While those concerns have largely been allayed, the work described here may suggest worthwhile directions for further research and development.

The near-bottom downforce experienced by a submerged submarine may present a manoeuvring problem since, without a hydrostatic restoring force and moment, control surface deflections are required to maintain clearance from the sea floor. On the surface, squat is the combination of sinkage and trim of a ship submarine while underway. It brings a likelihood of grounding in shallow water, where the additional downforce due to proximity of the bottom exacerbates the problem. In both cases the forces involved can be calculated by integrating dynamic pressure over the wetted surface of the vessel, and squat can then be obtained from basic hydrostatics. In principal a similar procedure can be applied to canal bank and ship-ship interactions, although accurately modeling the free surface becomes an additional concern. Of the two topics considered here, squat has received the most attention in the literature.

Using a number of standard methods, George [1] has predicted squat for current CF surface warships; he also summarises and compares the methods employed. Most of them are semiempirical or entirely empirical and, nominally at least, restricted to a limited range of hullform parameters. Sierra *et al* [2] discuss the effect of variable depth, and provide a comprehensive bibliography of squat and other aspects of operation in confined water. Tuck [3] authored a general analytical solution based on potential flow about a slender hull in shallow water (with, however, some limitations regarding slenderness and shallowness) that provides the general form of most of the semiempirical methods:

$$s = H \frac{F_h^2}{G} \quad (1)$$

where s is squat at some location, e.g., AP, midships, or FP; H is a function of vessel geometry; and G is a function of the depth Froude number $F_h = U/\sqrt{gh}$, where U is ship speed and h is depth of the undisturbed water. G is finite as $F_h \rightarrow 0$, and typically equal to about 1.0. Equation (1) applies to the region of practical interest for confined water operation, the subcritical region where $F_h < 1$. Tuck's method has been extended in a number of papers, e.g., reference [4]. Gourlay, a student of Tuck, further built on this work in an extensive review of analytical methods, including calculation in the transcritical regime and for non-uniform depth [5].

Standard methods for predicting squat generally do not explicitly break the problem down as suggested above, i.e., prediction of the hydrodynamic forces followed by a hydrostatic calculation, and are not applicable to the estimation of near-bottom downforce on a submerged submarine. Tuck and derivative methods are an exception, but they are restricted to shallow water: $h/T \leq 2$, where T is draft.

The procedure described here breaks the problem down as required, with forces obtained by solving for the potential flow numerically, rather than analytically, using the classic boundary integral method of a Rankine source distribution on the discretized hull [6]. An outline of the calculations is given in section 2; however, a number of their attributes are summarized below:

- Vessel representation is fully three-dimensional — slenderness is not an assumption. Speed is constant.
- Potential flow inherently neglects boundary layer growth and separation, but corrections can be made for thin boundary layers.
- Canal banks and other vessels are not represented.
- The free surface (in calculating forces on the surfaced submarine) is represented as a symmetry plane, or rigid streamline; this is a low Froude number assumption analogous to the double-hull ship models sometimes used in wind tunnels.
- The sea bottom is represented by a symmetry plane in which the vessel is reflected; any uniform depth of water, up to infinite depth, can be accommodated. However, the scope of this study did not permit modeling the multiple reflections that occur with both bottom and surface symmetry present, so they were neglected.
- The forces are not recalculated accounting for squat — a couple of trials suggested that this was not necessary. However, the hydrostatics of surfaced submarines should properly account for squat as noted below. Ideally, the whole sequence of calculations would be done iteratively.

While this approach provides almost all the capability suggested by George for a 3-D method [1], it is an exploratory study and the various components of the calculation have not been optimized or organized into an integrated package. Ways of mitigating some of the limitations and assumptions are discussed in the following sections.

There are very few relevant data in the open literature for validating either near-bottom or squat calculations for submarines, and the amount of validation done for the present study was limited. Some comparisons of the suggested method with data and with other predictions are presented in section 3 for the near-bottom force, and in section 4 for squat.

2 Calculation Methods

2.1 Potential Flow

Potential flow is calculated with the PC967 suite of programs, which is a revision of the first-order boundary integral code EN967 acquired some years ago for general 3-D flow calculations [7] and integrated into a more extensive ship hull flow procedure [8]. The latter has been superseded by the HLLFLO code [9].

The vessel is discretized into quadrilateral and triangular panels each having an associated source strength and a control point at which the boundary condition of tangential flow is enforced. The flow potential Φ , which is a function of the unknown source strengths, must satisfy the Laplace equation in the flow domain, $\nabla^2\Phi = 0$. The equivalence between potential flow and the discrete model is sketched in figure 1; a detailed discussion of boundary integral methods can be found in Hunt [6].

PC967 treats the vessel geometry as a series of components. These can include lifting appendages, i.e., sternplanes, as well as the hull. However, since the effect of a boundary can be neglected for a lifting surface more than one chord length away, only the hull was modeled. Figure 2 shows, for a notional hull section, how this was done for the three configurations of interest here. To simplify the figure, the waterline is shown at the equator of the section; if this is not the case, the geometry may have to be modified as discussed below. The components coloured black in the figure are input explicitly, and the green image components are accounted for by making the bottom a plane of symmetry.

A slightly modified approach can be taken with channel flows by discretizing not only the wetted surface of the vessel, but also the channel bottom and sides, and the free surface. The flowfield being a finite rather than infinite domain introduces some numerical complications including Kelvin sources on the free surface and the requirement to match conditions at the waterline. If undertaken, it would be most effective to implement this capability in HLLFLO [9] rather than the older codes.

Results are presented here in standard submarine coordinate axes and notation; see the Nomenclature and reference [10]. In particular, vertical force and displacement are positive downwards, and pitch angle is positive bow up (i.e., sinkage and trim by the stern are both positive). This coordinate system is different from that used in PC967 and from that generally used in ship hydrodynamics, so some care is required when comparing with results from other sources.

2.2 Hydrostatics

The squat of a conventional ship hull in response to a vertical force Z and pitching moment M can be estimated using linearized hydrostatics [11]. Sinkage Δz , which is implicitly determined at the LCF (x_{CF}), and trim $\Delta\theta$ are given by

$$\Delta z = \frac{Z}{\rho g A_{WP}} \quad (2)$$

$$\Delta\theta = \frac{M}{\rho g I_L} \quad (3)$$

where A_{WP} is the waterplane area and I_L is the waterplane moment of inertia; M and I_L are relative to the LCF. The principal assumption is that the vessel is essentially wall-sided at the waterline. This is indeed more likely to be the case for ships than for surfaced submarines. In particular, determination of $\Delta\theta$ with equation (3) implies

that the vessel is wall-sided at the fore and aft ends, and consequently the linearized formulation is questionable for a number of configurations including surfaced submarines with the fore and aft ends submerged and surface ships with shallow transom sterns.

From nonlinear hydrostatics, the sinkage and trim are solutions of the simultaneous integral equations

$$Z + \rho g \nabla = \rho g \int_{\text{AP}}^{\text{FP}} A(x, \Delta z, \Delta \theta) dx \quad (4)$$

$$M - \rho g \nabla x_{\text{CF}} = \rho g \int_{\text{AP}}^{\text{FP}} x A(x, \Delta z, \Delta \theta) dx \quad (5)$$

where ∇ is the zero-speed immersed volume and $A(x, \Delta z, \Delta \theta)$ is the immersed section area distribution for sinkage Δz and trim $\Delta \theta$. Equations (4) and (5) can be solved straightforwardly with standard numerical techniques. For this study, the hydrostatic calculations were programmed with Mathcad; example worksheets are given in annexes A and B.

3 Comparison of Near-Bottom Loads

3.1 Sphere Moving Parallel to a Boundary

PC967 calculations were initially done for an isolated sphere, i.e., in an infinite flow field, using 288 and 648 panels (corner points every 15 and 10 degrees respectively). These configurations are shown in figure 3. Because of symmetry, the surface pressure coefficient c_P is a function of the x coordinate alone. The classical doublet model [12], which is analytically exact for potential flow about an isolated sphere, gives

$$c_P(x) = 1 - \frac{9}{4} \left[1 - \left(\frac{x}{a} \right)^2 \right] \quad -a \leq x \leq a \quad (6)$$

where a is the radius of the sphere. Predictions of c_P are in very good agreement with the analytical solution, figure 4. Use of a higher panel density is not justified by this example.

The downforce coefficient c_Z for a doublet equivalent to a sphere of radius a moving above and parallel to an infinite plane at height h is equal to

$$c_Z = \frac{3}{8} \left(\frac{a}{h} \right)^4 \quad a < h \quad (7)$$

based on frontal area πa^2 [12]. While equation (7) is a good approximation for real spheres at moderate clearances, it ceases to be so at small clearances since the boundary condition that the surface of the sphere is a streamline is no longer enforced by the doublet model. Using a reflected image of the sphere, PC967 maintains

boundary conditions both on its surface and at the location of the plane, resulting in a coefficient that correctly approaches infinity as h/a approaches 1.0, figure 5.

The rapid increase in downforce at small clearances is further illustrated by plotting the pressure coefficient round a transverse cross-section close to the center of the sphere, figure 6. It can be seen that the upper surface of the sphere has a very small incremental effect on the downforce, even at very small clearances.

The characteristics of a somewhat submarine-like hull can be illustrated by the addition of parallel midbody. Figure 7 depicts 288-panel spheres stretched by midbody of length $2a$, where in one case the midbody is represented as one section with high aspect ratio panels and in the other by eight sections so that the midbody panels have similar dimensions to adjacent panels on the hemispherical end-caps. The axial pressure distribution for these in isolation shows a drastic decrease of the suction (negative c_p) peak at maximum radius compared with the original sphere, figure 8. However, a level of reduced suction is maintained along the midsection, and the accelerated flow that this represents is a major contributor to generating a near-bottom force. Figure 9 illustrates how the downforce in the proximity of a plane is increased for a stretched *vs.* unstretched sphere.

3.2 Submarine Model Experiments

In reference [13] Byström and Andersson describe captive near-bottom experiments with a model of the A17 submarine (Västergötland class). Data in that paper were sanitized by omission of the ordinate axis scale from the graphs, so this memorandum makes primarily qualitative comparisons. The PC967 calculations were done using a representative hull (the overall dimensions are in proportion, but the tail is probably fuller than the prototype) with 30 panels longitudinally and 24 around, figure 10.

Reference [13] plots the experimental loads against $2r/c$, where r is maximum hull radius and c is clearance between the keel and the tank bottom. Data for level trim, corresponding to the upper and lower parts of figure 6 in reference [13], are shown in figures 11 and 12, where the data and PC967 calculations have been adjusted to give reasonable overall agreement. These figures also include linear fit lines suggested in reference [13] for modeling the near-bottom effect in the equations of motion. Despite scales not having been optimally matched, the form of the PC967 curves characterizes the data better than the linear relationship, although neither captures very well the trend with $2r/c$ seen in figure 12.

The same data and PC967 predictions are plotted in figures 13 and 14, using the same relative ordinate scales as before, against h/r , where r is maximum hull radius. Since h/r is equivalent to h/a in section 3.1, figure 13 is analogous to figures 5 and 9. Presented in this fashion, comparisons between the data and potential flow appear more reasonable, while the anomalous behavior in measured pitching moment as $h \rightarrow r$ is more evident. Following the form of equation (7), the near-bottom downforce

coefficient can be represented by

$$Z' \propto \left(\frac{h}{r}\right)^{-n} \quad (8)$$

where Z' is based on L^2 [10] and L is hull length, with a similar expression for the pitching moment coefficient M' . Since n is unaffected by scaling the loads, estimates of it can be derived from figures 13 and 14:

	Z'	M'
	Figure 13	Figure 14
Reference [13] data	2.8	1.2 to 2.2
PC967 prediction	2.3	3.0

The indicated range of n for M' data was obtained by including or omitting the anomalous pitching moment measurements. Ignoring the anomaly, the near-bottom effect on a submarine can be modeled by equation (8) and its M' equivalent with, as a rough rule of thumb, $2 \leq n \leq 3$. The potential flow method outlined here should be able to estimate both n and the constant of proportionality reasonably well, but experimental corroboration is required to accurately model a specific submarine.

4 Comparison of Squat Results

4.1 CPF in Deep and Shallow Water

Since there are very few suitable squat data for submarines, this section presents a discussion of some results obtained for the Canadian Patrol Frigate (CPF).

The ship was taken to be in Deep Departure condition with FP draft of 4.99 m and AP draft of 4.95 m, corresponding to the model experiments described in reference [14]. The wetted surface, Component 1 in the notation of figure 2, and its image, Component 2, are represented in PC967 by 20 panels longitudinally and 12 panels around the girth; i.e., their corner points are defined at 21 equally spaced stations in 15 degree increments. The paneling is shown in figure 15. Hydrostatic calculations are illustrated by annex A.

The simple squat model represented by equation (1) clearly does not apply to deep water since it is zero in the limit $h \rightarrow \infty$. Deep water squat is therefore plotted against speed or the conventional hull length Froude number $F_r = U/\sqrt{gL}$. Figure 16 compares some predictions with scaled-up model test data. The notable feature of the measurements is a reversal from bow down trim at low speeds to much larger bow up trim at $F_r \approx 0.4$ ($U \approx 25$ kt), which is not predicted by either the linear or nonlinear

hydrostatic calculations. The figure also shows that the linear and nonlinear predictions give about the same sinkage but that trim is markedly less bow down in the nonlinear prediction, presumably due to the lack of wall-sidedness at the fore and aft ends.

In the absence of data for shallow water squat, some comparisons were made with the methods discussed in reference [1]. Unfortunately, the key figures in that reference, e.g., figure B-1-1, are not suitable for direct comparison since the trim, and whether maximum squat is at the FP or AP, are not noted. The effect of water depth on the longitudinal distribution of downforce calculated by PC967 for the CPF is illustrated in figure 17. Squat predictions were compared with the methods of Vermeer [15] and Millward [16].

Vermeer's method is based on that of Tuck [3]:

$$\Delta z_{\text{MID}} = c_z \frac{\nabla}{L^2} \frac{F_h^2}{\sqrt{1 - F_h^2}} \quad (9)$$

$$\Delta \theta = c_\theta \frac{\nabla}{L^3} \frac{F_h^2}{\sqrt{1 - F_h^2}} \quad (10)$$

where Δz_{MID} is sinkage at midships. He simplified Tuck's analytical derivation of the coefficients c_z and c_θ by approximating the waterplane curve $B(x)$ and area curve $S(x)$ by

$$B(x) = (1 - x^2) (1 + \alpha_B x^2 + \beta_B x^3) \quad (11)$$

$$S(x) = (1 - x^2) (1 + \alpha_S x^2 + \beta_S x^3) \quad (12)$$

in which α_B , β_B , α_S , and β_S are functions of LCF, longitudinal center of buoyancy LCB, and waterplane and prismatic coefficients, C_W and C_P respectively. For shallow water of infinite extent, Vermeer obtained:

$$c_z = \frac{1}{6\pi C_W C_P} [32 - 40(C_P + C_W) + 75 C_P C_W - 980 C_P C_W C_B C_F] \quad (13)$$

$$c_\theta = \frac{-7}{18\pi C_W C_P k_W^2} [(20 C_P - 45 C_P C_W) C_B + (24 C_W - 39 C_W^2) C_F] \quad (14)$$

where k_W is longitudinal radius of gyration of the waterplane and C_F and C_B are the LCF and LCB nondimensionalized by L . He gives similar expressions for sinkage and trim in a finite channel [15]. Vermeer's approximations to the CPF waterplane and area curves are shown in figure 18; it can be seen that equations (11) and (12) assume a cruiser, rather than transom, stern.

From a large number of towing tank tests with commercial ship models in shallow water of effectively infinite extent, Millward obtained empirical expressions [16] for squat at midships (s_{MID}) and at the bow (s_{BOW}) in the form of equation 1:

$$s_{\text{MID}} = \left(12.22 C_B \frac{B}{L} - 0.46 \right) \frac{F_h^2}{1 - 0.9 F_h} \quad (15)$$

$$s_{\text{BOW}} = \left(15.0 C_B \frac{B}{L} - 0.55 \right) \frac{F_h^2}{1 - 0.9F_h} \quad (16)$$

where B is the beam at midships. The range of validity of these expressions is stated to be $1.25 < h/T < 6$.

Figures 19 and 20 compare linear estimates of AP and FP squat from the present method with calculations from Vermeer’s and Millward’s methods. There is clearly a considerable difference between all three. Vermeer gives somewhat less sinkage, and significant bow up trim, compared with the modest bow down trim predicted by Millward; this is consistent with George’s figure 3–6 [1]. Since the present method accounts for depth and speed separately, not combined into the single parameter F_h , it generates a family of curves when squat is plotted against the depth Froude number, as seen in these figures. The “fit to linear estimate” curves are locally weighted regressions of both the $h = 8$ m and 12 m estimates. These curves indicate a predicted bow down trim similar to Millward with somewhat less sinkage — more like that suggested by Vermeer. Without data for shallow water squat it is not possible to resolve the discrepancies between these predictions.

4.2 Submarine in Shallow Water

In reference [17], Eddison and Fryer describe a study of surface manoeuvring in confined water for the SSBN05 (Vanguard) class submarine. The study included model scale measurements of squat in shallow water.

The draft of a surfaced submarine is typically at least 80 percent of pressure hull diameter, as shown in the left-hand sketch of figure 21, rather than 50 percent as suggested by figure 2. Paneling the hull and its reflected image to the waterline causes difficulty for the potential flow calculation; errors arising from proximity of hull and image panels at the waterline, and from an unrealistic local surface boundary condition, may become large relative to the contribution of the upper hull as the draft increases. To mitigate these problems, in potential flow calculations the lower hull was joined to its image by vertical panels at the maximum beam, as shown in the center and right-hand sketches of figure 21. Although this effectively determines downforce and pitching moment from just the lower hull and image contributions to it, the approximation is considered acceptable.

Figure 22 shows paneling arrangements for an axisymmetric hull representing SSBN05 general proportions, and the corresponding modified hull and image for surfaced downforce and pitching moment estimation. Notwithstanding the geometric modification required for PC967, hydrostatic calculations were done with the actual geometry, see annex B.

The bare hull geometry is normally sufficient for near-bottom or squat force calculations. The effect of including a keel was investigated for this hull by calculating the deep water near-bottom force for the bare hull and with a 1 m deep, 2 m wide keel added along the parallel midbody, about 57.5 percent of total hull

length. Height above the bottom, h , was set at 8.4 m, giving a zero-trim clearance of 2 m for the bare hull and 1 m for the keel. The resulting downforce distributions are shown on figure 23. The difference in net downforce is less than four percent, while the keel brings the peaks of the distribution a little closer to midships, i.e., towards where it begins and ends. These differences do not justify modeling a keel even at very small bottom clearances. It was noted previously that it is not necessary to model cruciform configuration sternplanes, which are about one chordlength above the bottom at minimum clearance; studies of wings in ground effect, e.g., reference [18], show that the interaction at this distance is negligible. Interaction with lower X-rudders, on the other hand, might not be negligible.

The shallow water squat data in reference [17] are reproduced on figure 24. There is a considerable discrepancy between data for 1/40 and 1/26 scale models. Eddison and Fryer concluded that the latter incorporated excessive blockage effects, so they are not included in the comparisons below. It was observed that the models trimmed by the bow; however, the “estimated sinkage at CG” curve on the figure indicates that the trim angle was quite small. Reference [17] gives little detail on experimental conditions. In the comparisons presented here, squat estimates were made for the submarine initially in nominal deep draft condition with a trim of 0.7 degrees by the stern.

Although a surfaced submarine differs quite considerably from the hullforms on which the Vermeer and Millward methods are based, it is of interest to first compare predictions from those methods with the model data. Vermeer’s approximations to the waterplane and area curves, figure 25, are reasonable except near the stern, where, as the waterplane curve shows, the hull sections were fully submerged. Comparison with data for stern sinkage is shown in figure 26. Forward sinkage was predicted to be significantly higher than measured, and, as the mean sinkage approximates the estimate for the CG on figure 24, it appears that overprediction of trim by the bow is largely responsible for the discrepancies in this figure.

Potential flow calculations were done at model scale and full scale, modifying the hull geometry in each case by a boundary layer displacement thickness distribution derived for axial flow on the axisymmetric hull [19]. Displacement thickness δ^* is compared for model (1/40) scale at various full scale speeds and full scale at 2 kt in figure 27.

It was noted in the previous section that squat should be represented by a family of curves when plotted against depth Froude number. The predictions in figure 28 represent calculations done for $h = 10, 11, 12, 13, 14,$ and 15 m at 2, 4, 6, 8, 10, and 12 kt full scale, and scaled up to 6, 8, 10, and 12 kt for a 1/40 model. Model scale predictions are in reasonable agreement with the data, with the full scale stern sinkage predicted to be 20 to 25 percent lower.

Notwithstanding the similarity of model scale and full scale stern sinkage predictions in figure 28, forward sinkage agrees less well. This is because trim, although quite small, is predicted to be different in the two cases, figures 29 and 30. In figure 30, the model is predicted to trim by the stern while full scale trims by the bow at low speed

and at shallow depths, otherwise tending to trim by the stern. Further corroboration is required to establish whether this is a genuine scaling effect or an artifact of the calculation method.

5 Concluding Remarks

This memorandum records a brief study of estimating submarine near-bottom loads and surfaced squat by combining potential flow hydrodynamic forces with hydrostatic calculations. Squat estimates were compared with the standard methods (for surface ships) of Vermeer and Millward. The scarcity of suitable experimental data for submarines presents a problem for adequately validating both near-bottom and squat calculations.

Boundary integral calculation of potential flow near-bottom force was validated for a sphere moving parallel to the bottom and, with respect to the trend with clearance under the hull, for experiments with a submarine model, although absolute values for comparison were not available in the latter case. DRDC is planning near-bottom model experiments that will enable more detailed comparisons to be made. The principal test parameters will be clearance and trim angle; secondary parameters may include sternplane deflections and drift angle.

Squat estimates were compared with model data for the CPF in deep water and for a submarine in shallow water. Results obtained with the present method and other methods discussed here suggest that sinkage can in general be predicted at least more consistently, if not more accurately, than can trim. Nevertheless, accurate measurement of these quantities, particularly trim, is not easy even in well-conducted model experiments, which adds another element of uncertainty to comparisons and validation. Hydrostatic calculations for the submarine demonstrated scaling effects in squat; this should be investigated in future investigations since standard estimation methods rely heavily on model scale experimental data.

References

1. George, M. (2000). Squat Charts for Safe Navigation of CF Warships. (Project GEL-9905). George Engineering Ltd. LIMITED DISTRIBUTION.
2. Sierra, M.A.H., Rodriguez, R.Z. and Rojas, L.P. (2000). El Fenomeno Squat en Areas de Profundidad Variable y Limitada (1). In *II International Conference on Oceanic Engineering, Ocean 2000*. Valdivia: Universidad Austral de Chile.
3. Tuck, E.O. (1966). Shallow-Water Flows past Slender Bodies. *Journal of Fluid Mechanics*, Vol. 26, Part 1.
4. Tuck, E.O. and P.J. Taylor (1970). Shallow Wave Problems in Ship Hydrodynamics. In *Eighth Symposium on Naval Hydrodynamics*, Rome. Washington: Office of Naval Research.
5. Gourlay, T. (2000). Mathematical and Computational Techniques for Predicting the Squat of Ships. Ph.D. Thesis. University of Adelaide, Department of Applied Mathematics.
6. Hunt, B. (1980). The Mathematical Basis and Numerical Principles of the Boundary Integral Method for Incompressible Potential Flow over 3-D Aerodynamic Configurations. In *Numerical Methods in Applied Fluid Dynamics* (Hunt, B., ed.). London: Academic Press.
7. Mackay, M. (1986). Program EN967 – A Revised User Guide. (DREA TC 86/305). Defence Research Establishment Atlantic.
8. Mackay, M. and Hally, D. (1985). The Calculation of Potential Flow about Ship Hulls. (DREA TM 85/204). Defence Research Establishment Atlantic.
9. Hally, D. (1993). User's Guide for HLLFLO Version 2.0. (DREA TC 93/309). Defence Research Establishment Atlantic.
10. Gertler, M. and Hagen, G.R. (1967). Standard Equations of Motion for Submarine Simulation. (NSRDC Report 2510). Naval Ship Research and Development Center.
11. Clayton, B.R. and Bishop, R.E.D. (1982). *Mechanics of Marine Vehicles*. London: Spon.
12. Milne-Thomson, L.M. (1949). *Theoretical Hydrodynamics* (Second Edition). London: Macmillan.
13. Byström, L. and Andersson, R. (1996). Submarine Manoeuvring with a Small Bottom Clearance. In *Warship '96 International Symposium on Naval Submarines 5*. London: The Royal Institution of Naval Architects.

14. Cumming, D., Datta, I., and Molyneux, W.D. (1997). CPF Captive Model Tests using Hydro-Elastic Model M460, Parts 1 and 2. (IMD TR-1997-17 and -19). National Research Council Canada, Institute for Marine Dynamics. LIMITED DISTRIBUTION.
15. Vermeer, H. (1977). The Behavior of a Ship in Restricted Waters. *International Shipbuilding Progress*, Vol. 24, No. 280.
16. Millward, A. (1990). A Preliminary Design Method for the Prediction of Squat in Shallow Water. *Marine Technology*, Vol. 27, No. 1.
17. Eddison, J.F.P. and Fryer, D.K. (1991). Some Aspects of Submarine Behavior when on the Surface in Shallow Water. In *Warship '91 International Symposium on Naval Submarines 3*. London: The Royal Institution of Naval Architects.
18. Moore, N., Wilson, P.A., and Peters, A.J. (2002). An Investigation into Wing In Ground Effect Airfoil Geometry. In *RTO Meeting on Challenges in Dynamics, System Identification, Control and Handling Qualities for Land, Air, Sea, and Space Vehicles*. (RTO-MP-095). Paris: NATO RTO.
19. Truckenbrodt, E. (1955). A Method of Quadrature for Calculation of the Laminar and Turbulent Boundary Layer in case of Plane and Rotationally Symmetric Flow. (NACA TM 1379). National Advisory Committee for Aeronautics.

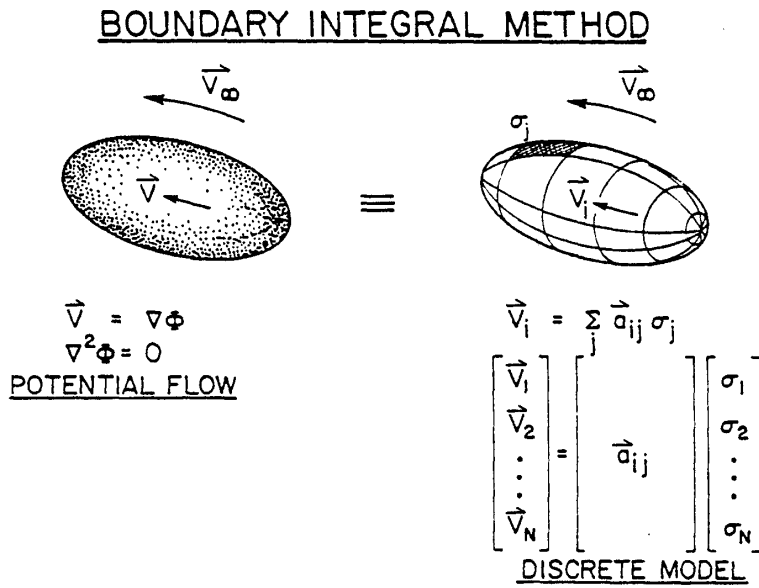


Figure 1. Equivalence of potential flow and the discrete model, from [8]. Freestream flow, equivalent to U in the text, is denoted V_∞ ; V and V_i are local velocity; a_{ij} are geometrically-determined influence coefficients; and σ_j are the source strengths.

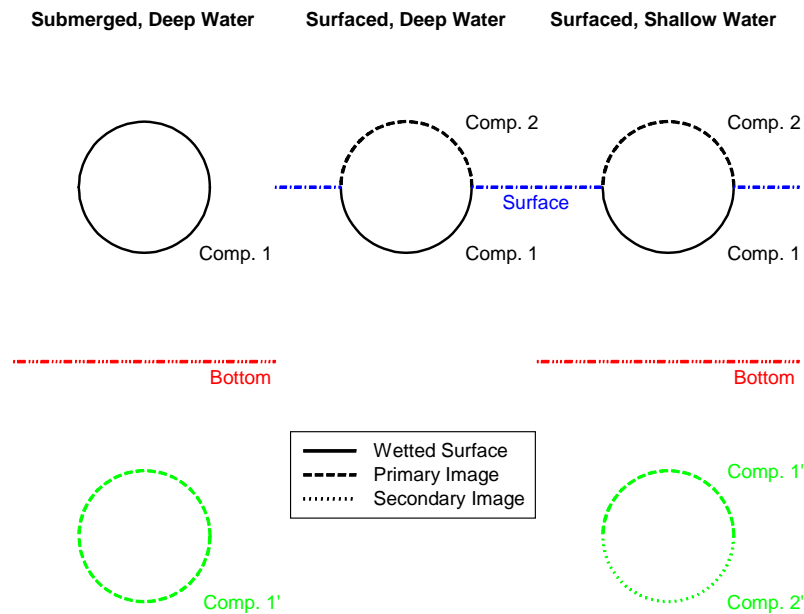


Figure 2. PC967 geometry setup for three configurations: submerged, deep water; surfaced, deep water; and surfaced, shallow water. For each, the calculation sums the contributions of all components to the force on Component 1.

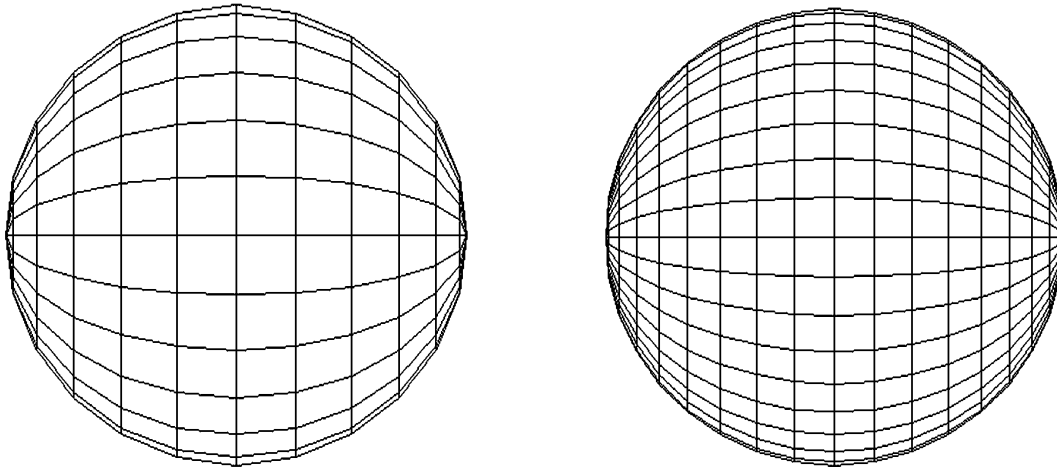


Figure 3. Sphere paneling: left, 288 panels; right, 648 panels. The x axis is horizontal.

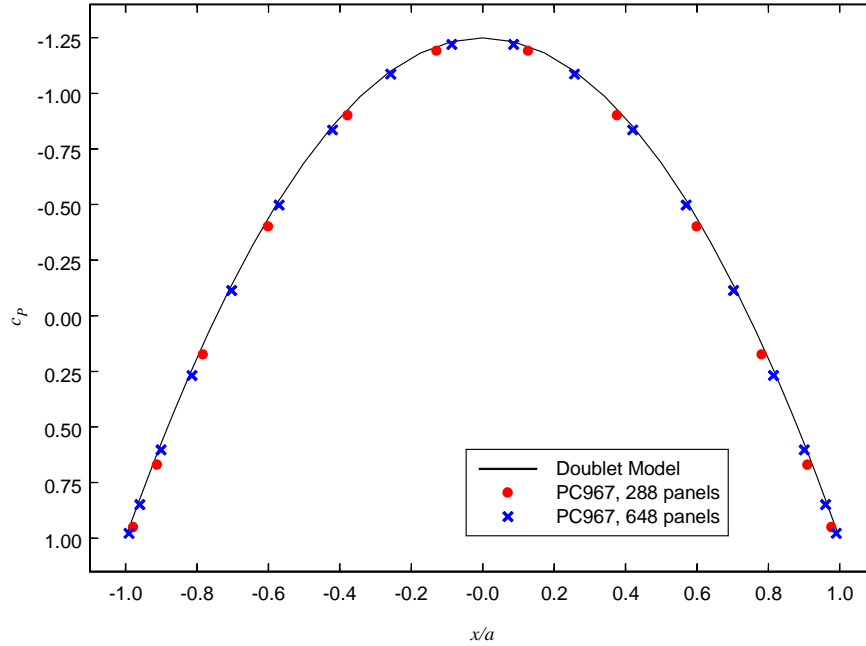


Figure 4. Axial pressure distribution on an isolated sphere.

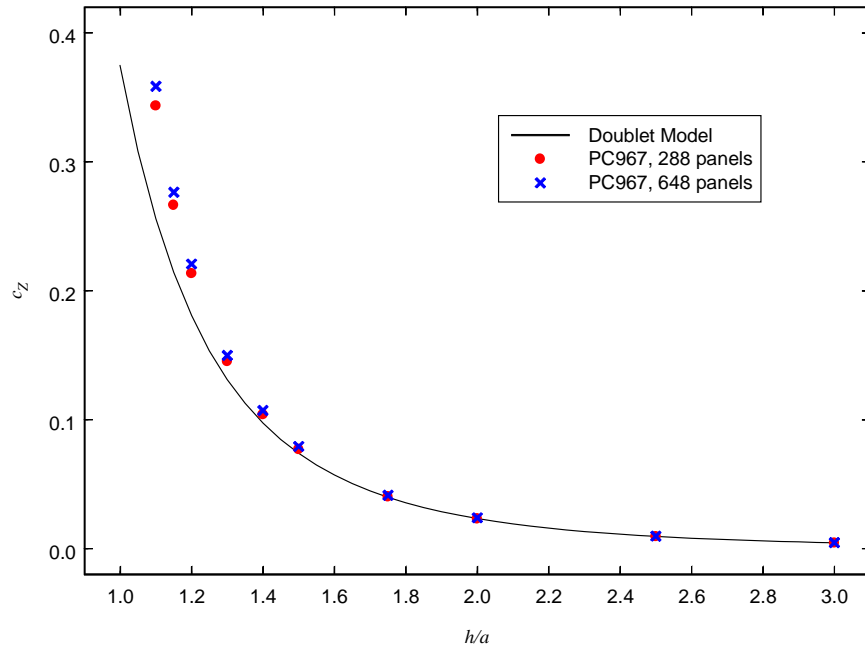


Figure 5. Force coefficient on a sphere moving parallel to a plane.

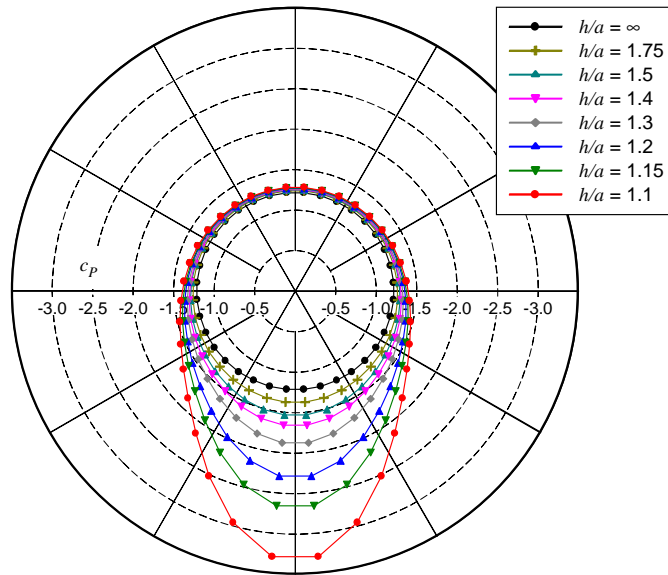


Figure 6. Pressure coefficient round the near-midsection of a 648-panel sphere moving parallel to a plane.

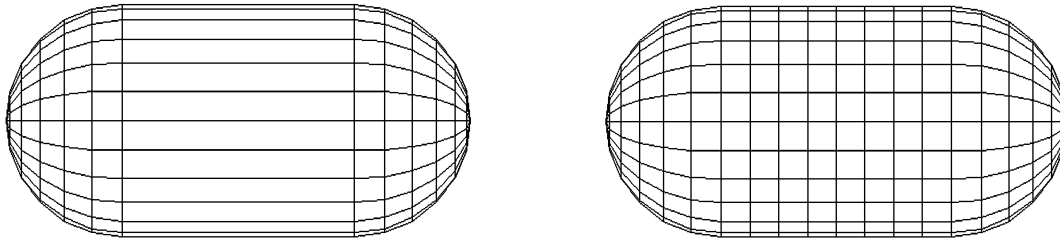


Figure 7. Stretched spheres (288+ panels): left, “1 panel” stretch; right, “8 panel” stretch. The x axis is horizontal.

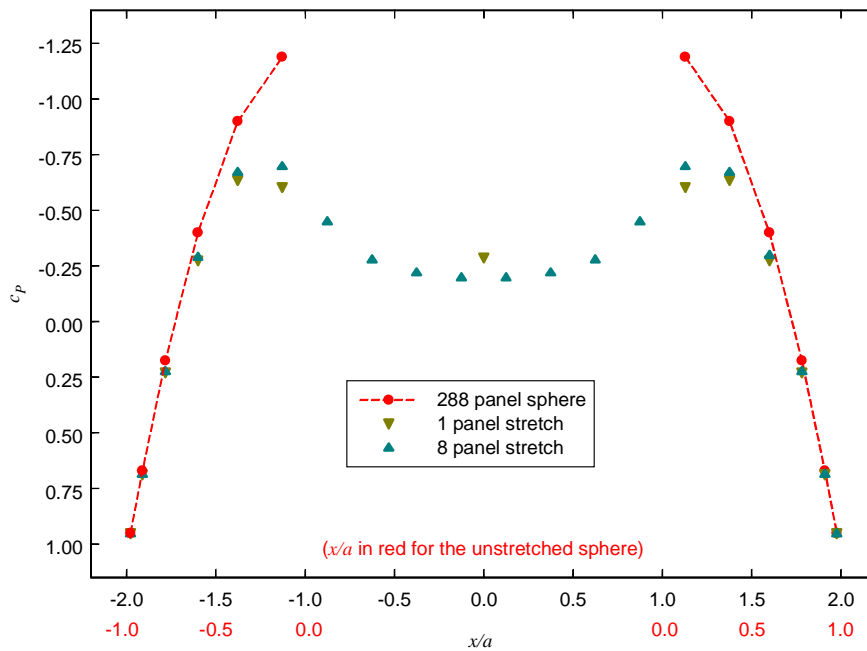


Figure 8. Axial pressure distribution on isolated stretched spheres.

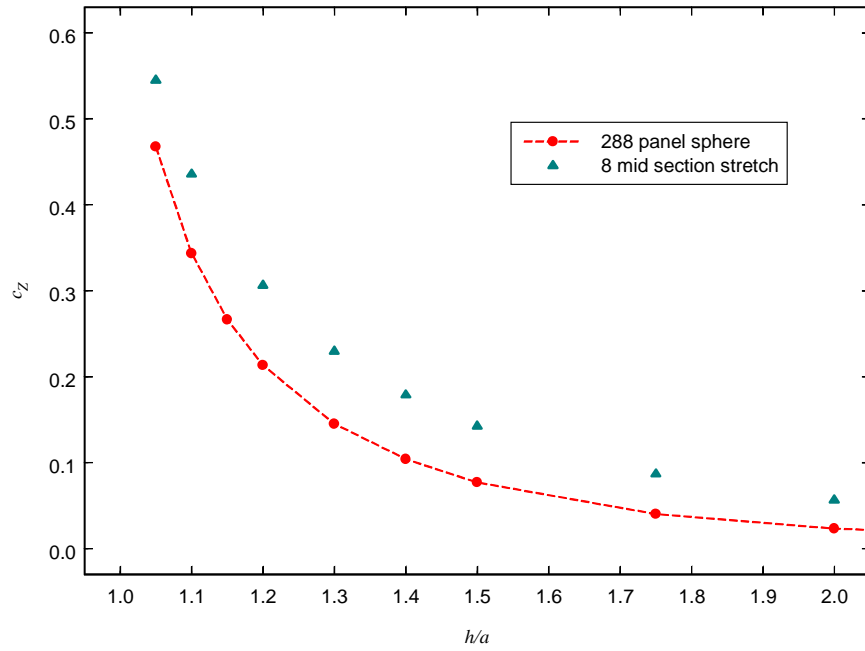


Figure 9. Force coefficient on a sphere and stretched sphere moving parallel to a plane.

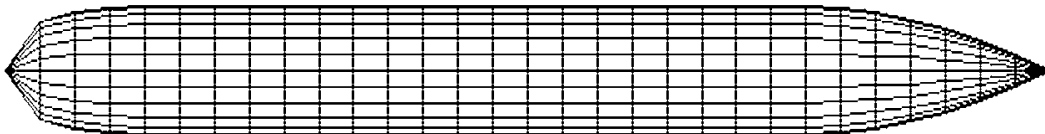


Figure 10. Representative hull for comparison with near-bottom model experiments [13].

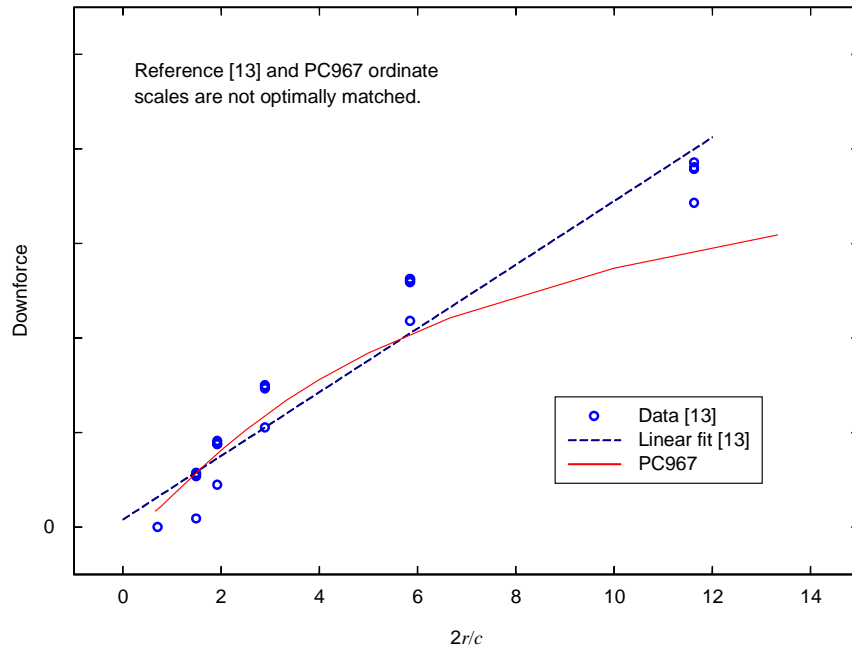


Figure 11. Submarine near bottom: downforce plotted against $2r/c$, as in reference [13], figure 6.

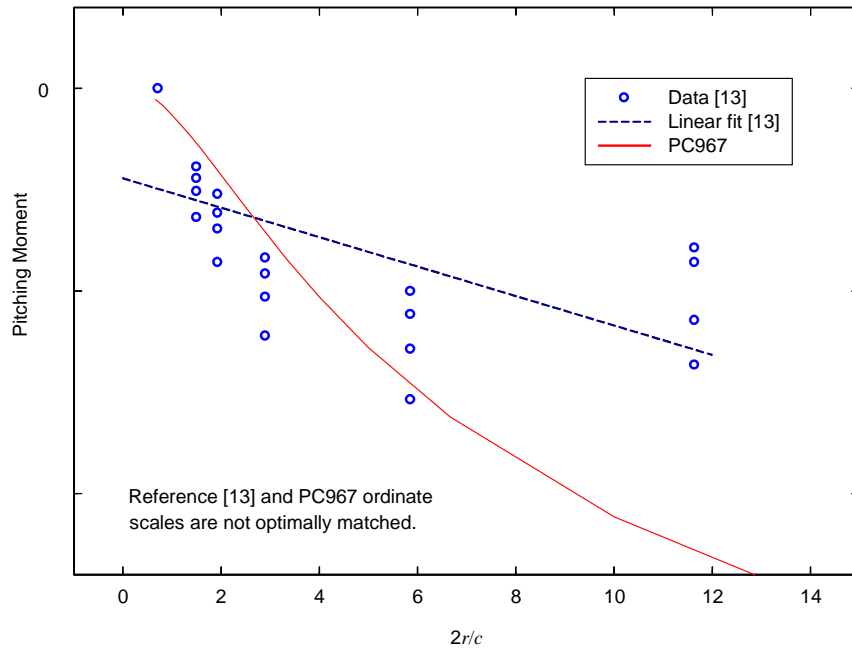


Figure 12. Submarine near bottom: pitching moment plotted against $2r/c$, as in reference [13], figure 6.

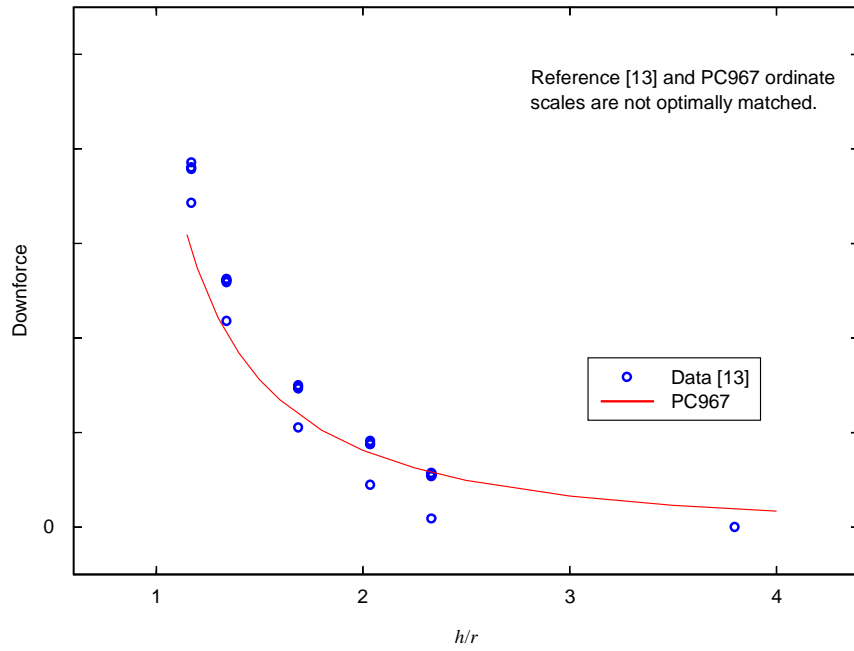


Figure 13. Submarine near bottom: downforce plotted against h/r .

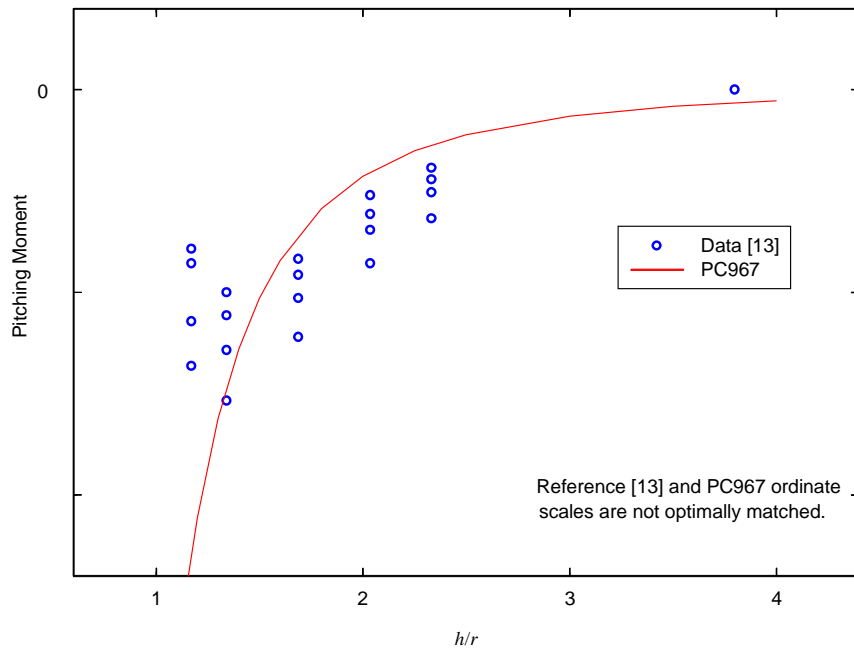


Figure 14. Submarine near bottom: pitching moment plotted against h/r .

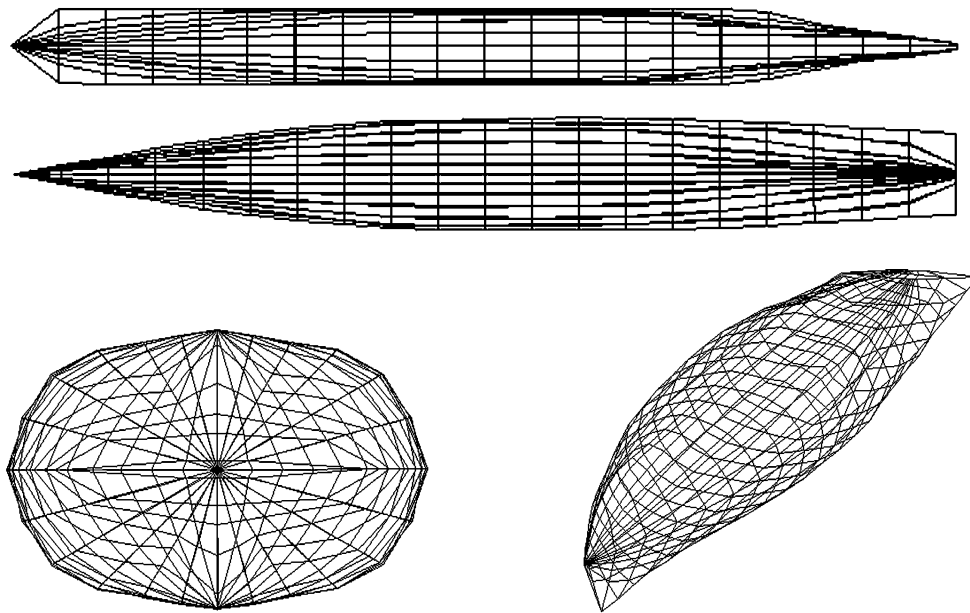


Figure 15. Paneling for the CPF hull and its image: top, side elevation; below, plan view; left, section plan; right, isometric view.

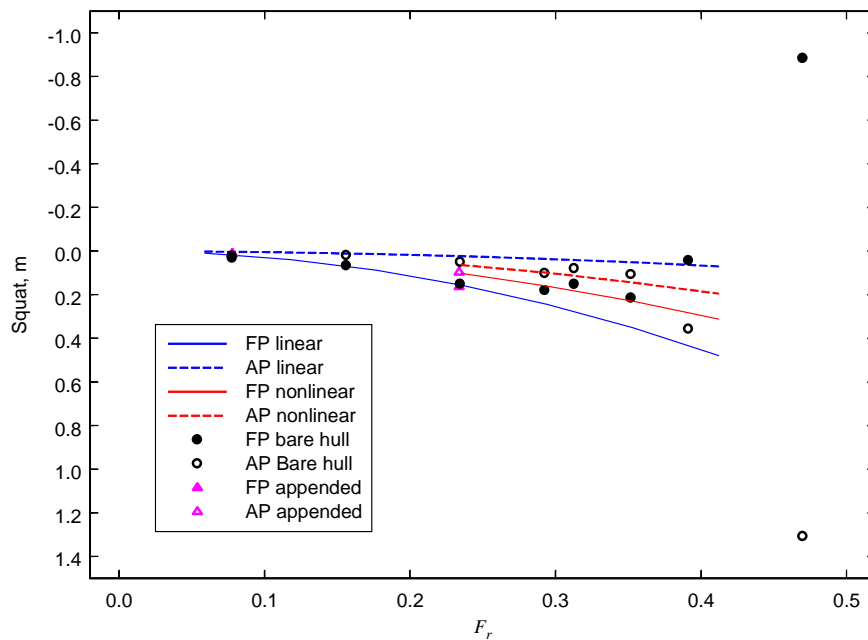


Figure 16. CPF deep water squat. The lines are predictions, the symbols are data from reference [14].

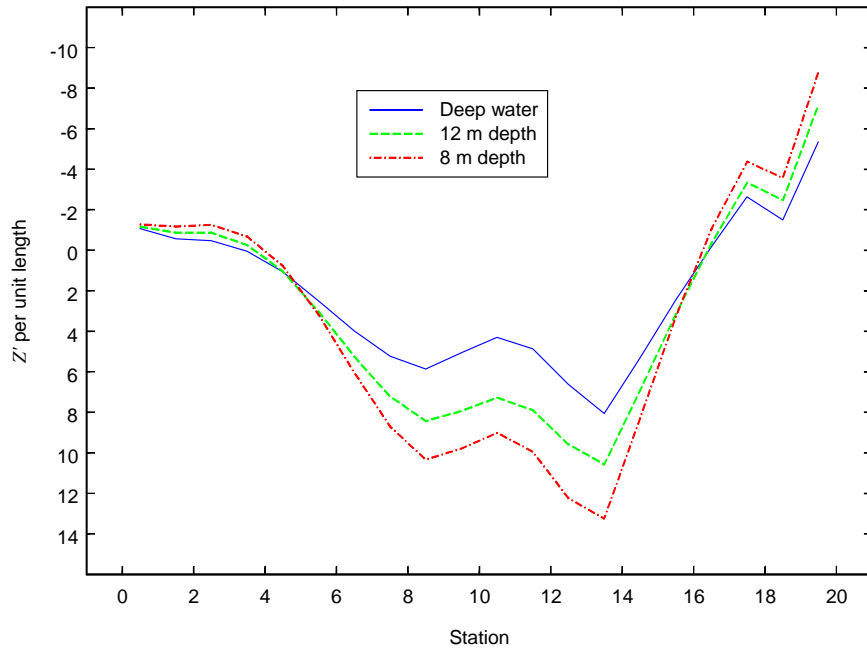


Figure 17. CPF: longitudinal distribution of downforce calculated by PC967 for $h = \infty$, 12 m, and 8 m. Here, and following, station 0 = FP and station 20 = AP.

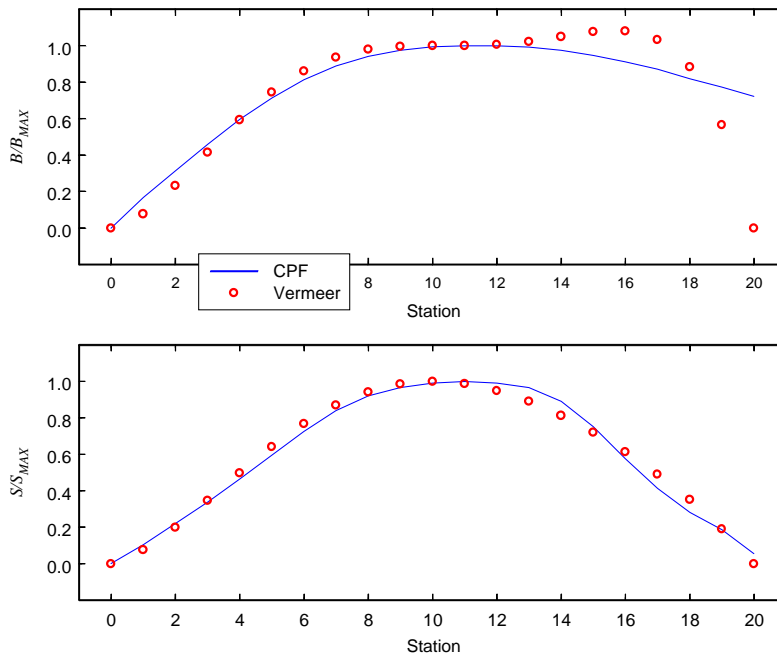


Figure 18. Nondimensional CPF beam and area compared with Vermeer's approximations (equations (11) and (12)).

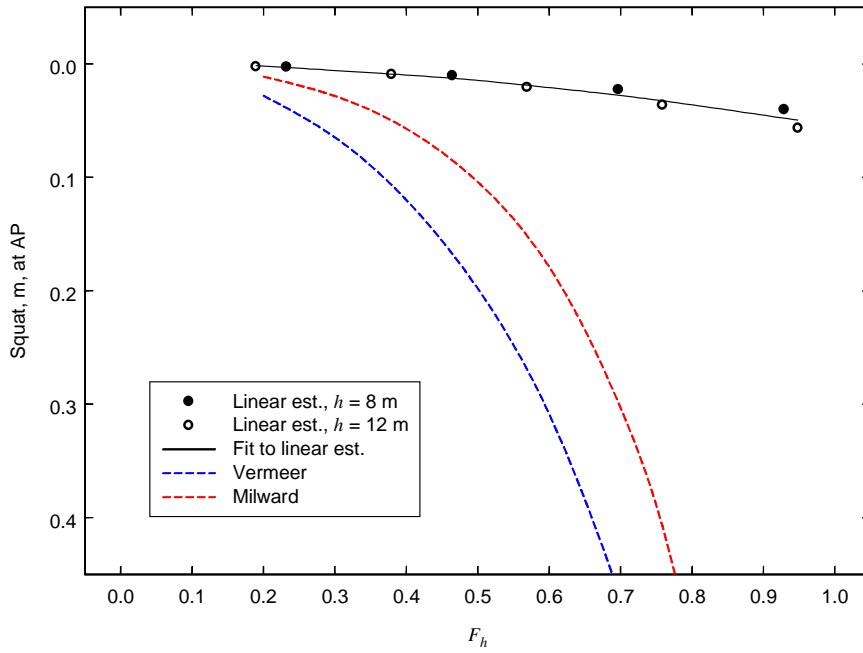


Figure 19. CPF: shallow water AP squat estimates.

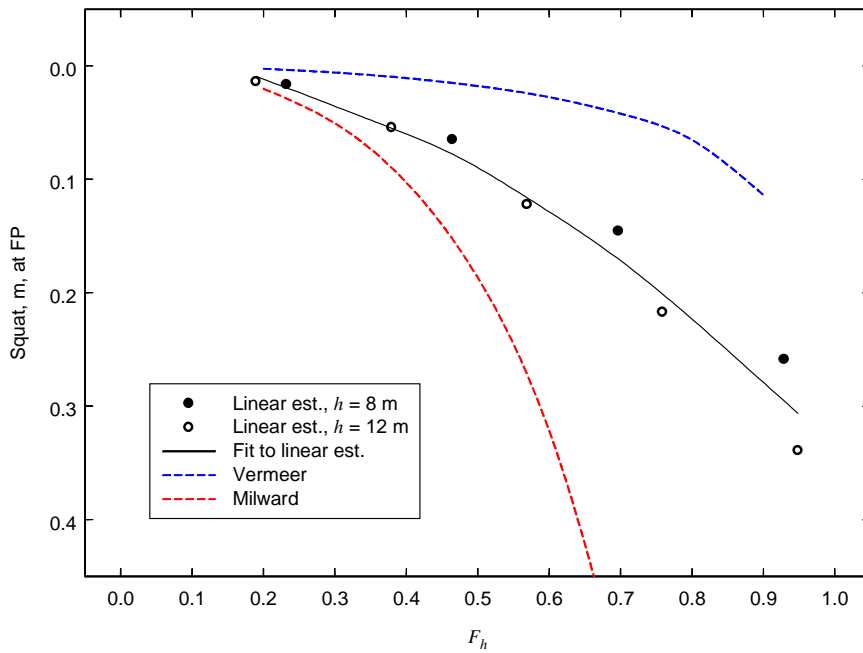


Figure 20. CPF: shallow water FP squat estimates.

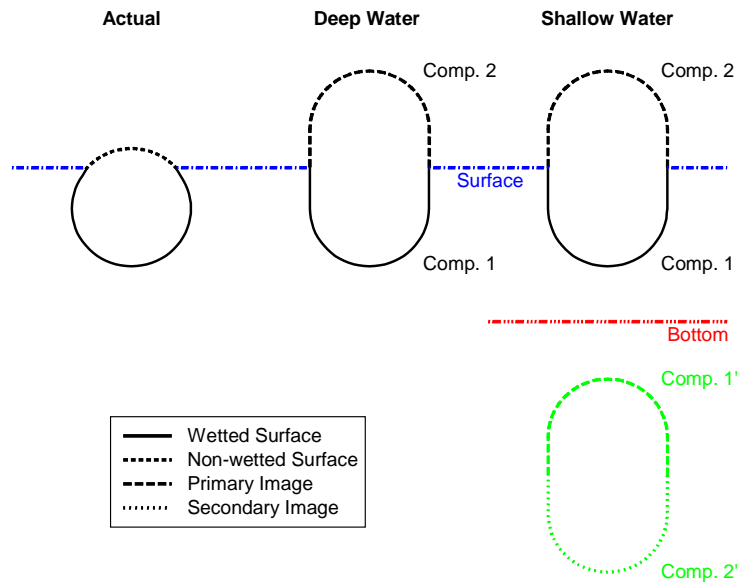


Figure 21. Actual geometry for a surfaced submarine hull, and PC967 approximations for deep and shallow water. The calculation sums the contributions of all components to the force on Component 1.

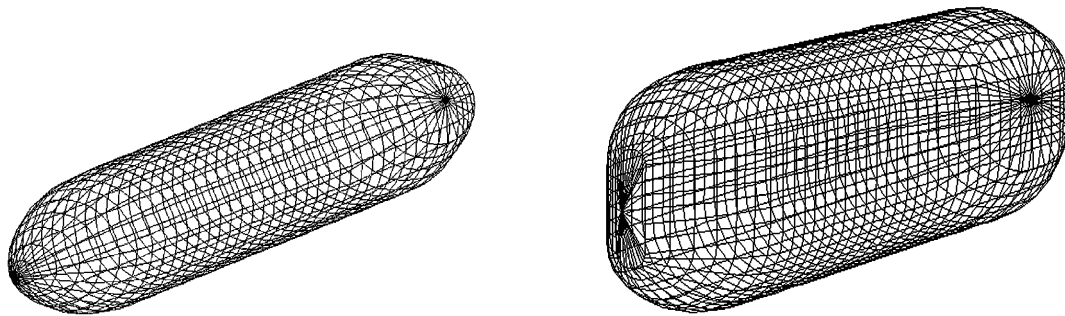


Figure 22. Submarine hull paneling for comparison with squat experiments: left, submerged, 24×40 panels; right, surfaced (with image), 36×40 panels.

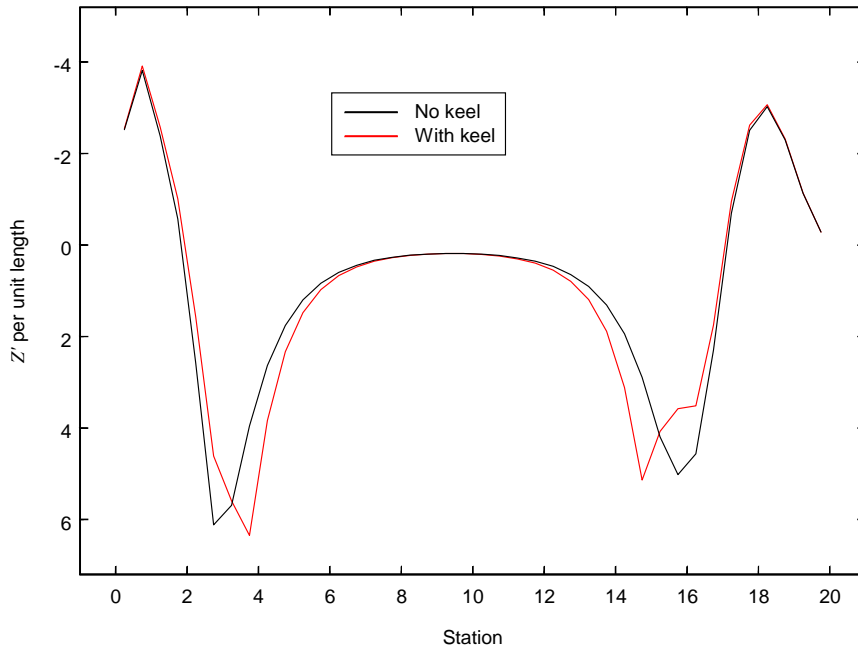


Figure 23. Longitudinal distribution of downforce estimated by PC967 for SSBN05 hull with and without a keel in deep water at $h = 8.4$ m.

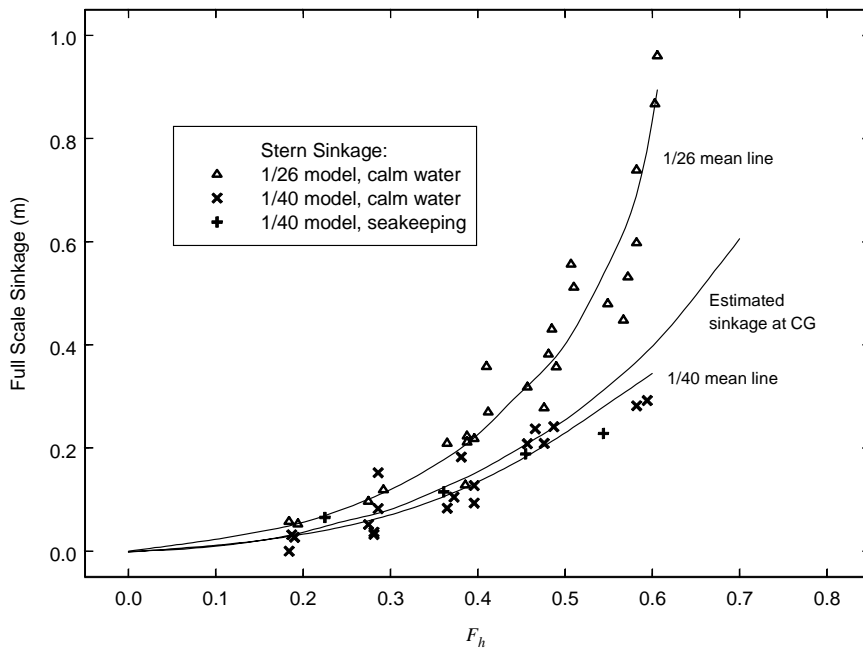


Figure 24. Submarine squat: sinkage data for SSBN05, from reference [17].

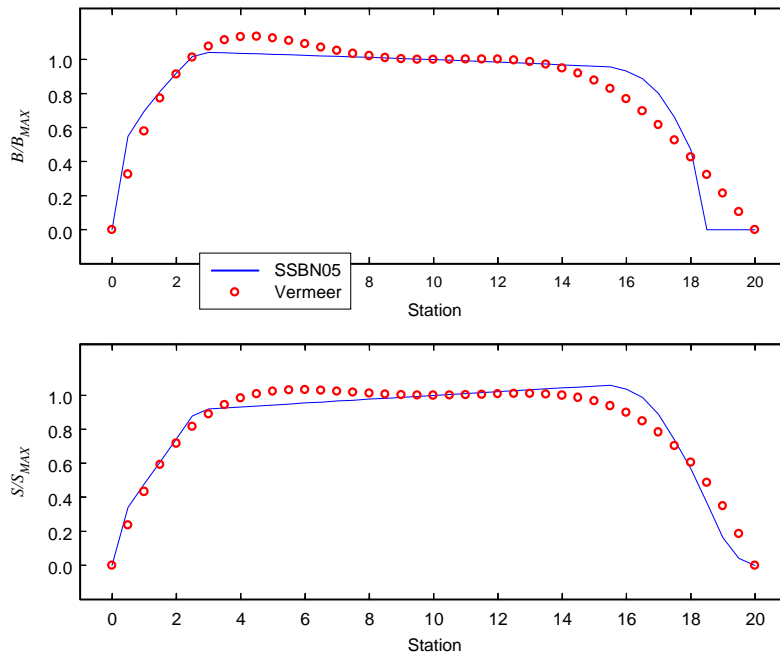


Figure 25. Nondimensional SSBN05 beam and area, in nominal surfaced deep draft condition, compared with Vermeer's approximations (equations (11) and (12)).

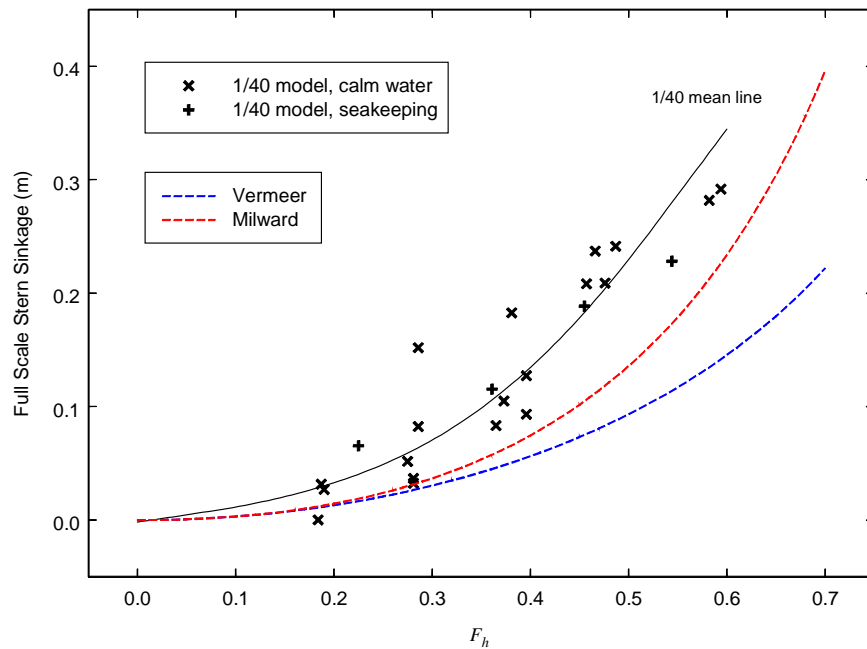


Figure 26. Submarine squat: comparison of SSBN05 model data [17] for stern sinkage with estimates from the Vermeer and Millward methods.

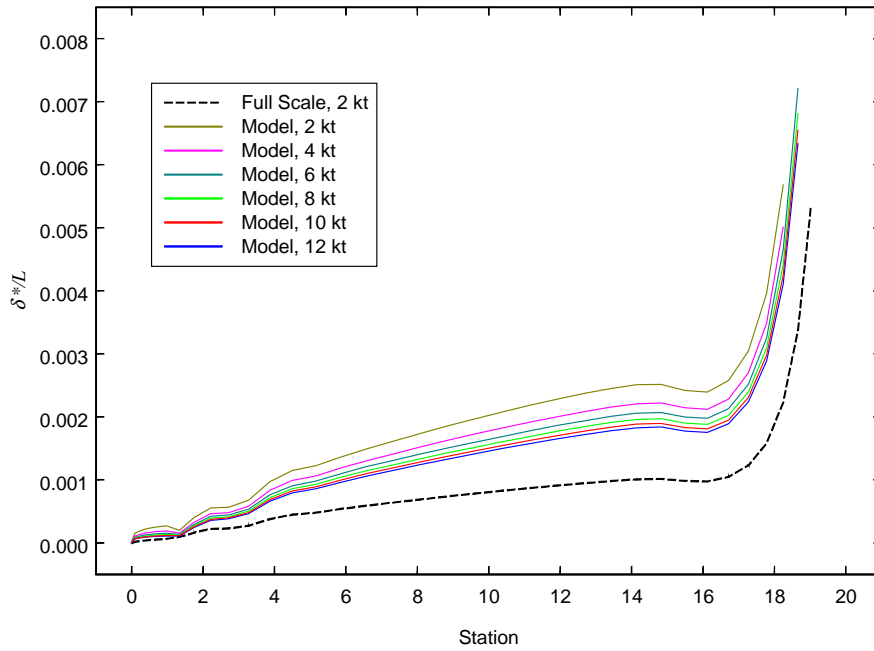


Figure 27. Estimated nondimensional boundary layer displacement thickness for SSBN05 hull in axial flow (deep water).

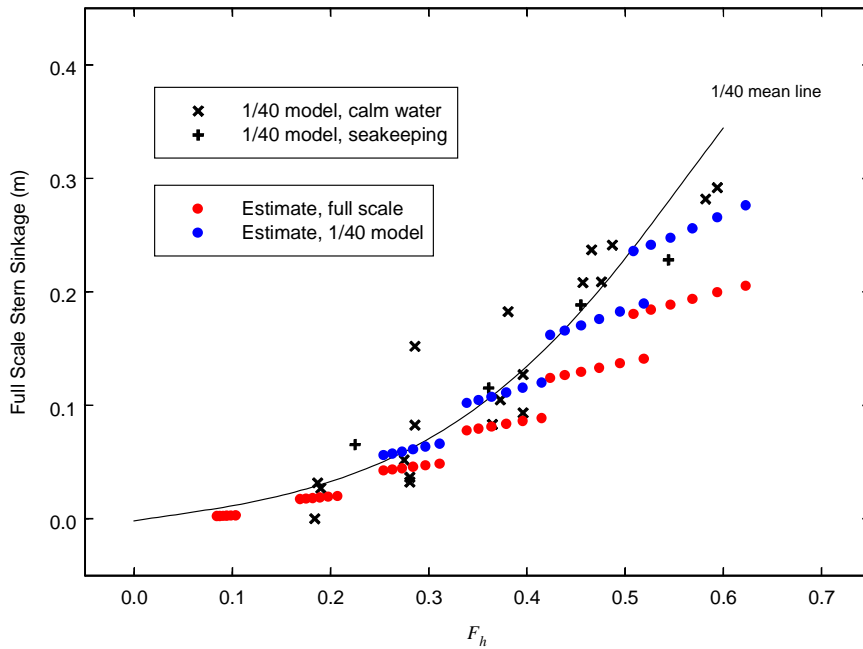


Figure 28. Submarine squat: comparison of SSBN05 model data [17] for stern sinkage with estimates at model and full scale from the present method.

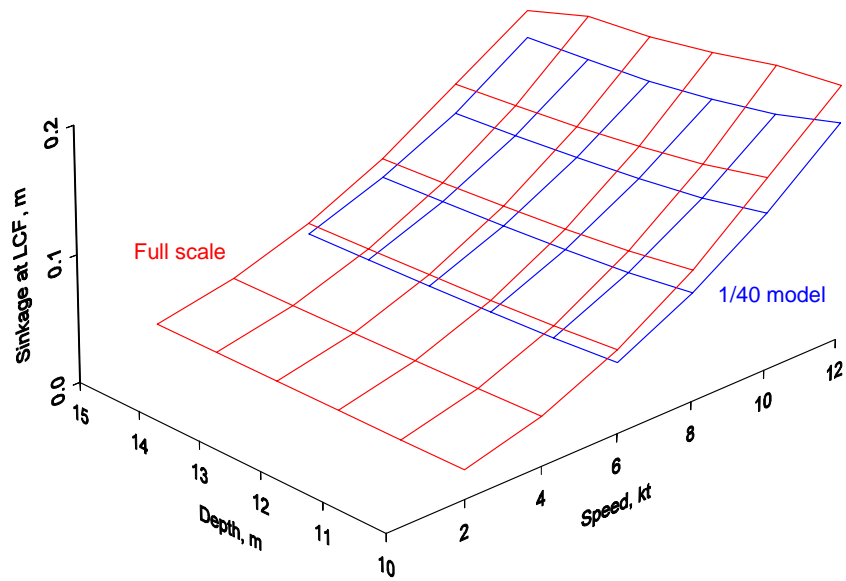


Figure 29. Submarine squat: predicted sinkage at LCF for SSBN05.

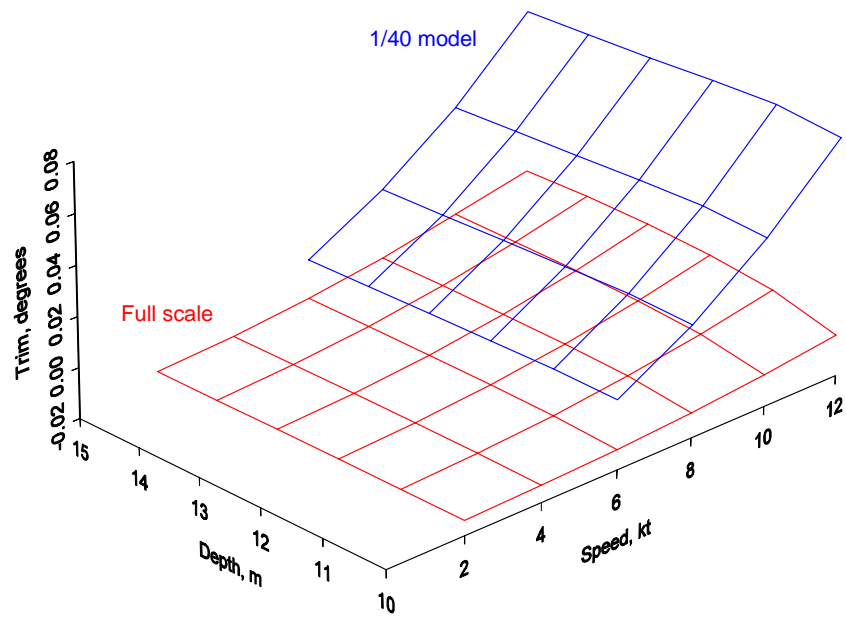


Figure 30. Submarine squat: predicted trim for SSBN05.

Annex A. Hydrostatic Calculation Worksheet for Surface Ship

With minor modifications, the procedure shown on the next five pages could be used for any surface ship. The worksheet is programmed in Mathcad 2000 (www.mathcad.com).

Hull geometry to the sheer line is entered into the input tables **YS** and **ZS** for 21 stations, starting at the AP. **ZS** is measured up from the keel line. Right-click within each table and select “Import” to read an ASCII file of values. Normal force and pitching moment from PC967, which are entered at the top of the third page of the worksheet, must be in standard submarine coordinates (Z downwards, M bow up).

Linear squat estimates are made with the calculation of two intermediate quantities: TPI (Tons Per Inch immersion – the name is a historical anachronism) and MCT (Moment to Cause Trim) [11]. The sinkage and trim are Z/TPI and M/MCT respectively.

In the iterated estimates, note that section area is obtained by integrating the interpolated section offsets. Consequently, the right-hand sides of equations (4) and (5), which are on the last page of the worksheet, are double integrals with internal computational overhead for interpolation and several function evaluations. This makes solving for Δz and $\Delta\theta$ very slow, and relatively few of these evaluations were done for the present study. The process would be considerably speeded up by generating a set of Bonjean (section area) curves prior to the calculation.

HALHULL_STAT2.MCD

Section Geometry:

YS :=

	0	1	2	3	4	5	6
0	0	0	0	0	0	0	0
1	2000	1000	148	178	341	1000	1000
2	3500	2000	1000	1000	759	1183	2000
3	5000	3000	2000	2000	1000	2000	3000
4	5434	3871	3000	3000	1716	3000	3437
5	5549	4000	4000	3293	2000	3085	4000
6	5630	5000	5000	4000	3000	4000	4896
7	5767	5807	5131	5000	4000	4787	5000
8	5924	5913	6000	5568	5000	5000	5777
9	6000	6000	6117	5892	5376	6000	6000

ZS :=

	0	1	2	3	4	5	6
0	4630	3670	2970	1880	517	0	0
1	4631	3739	3000	2000	1000	897	345
2	4632	3811	3153	2453	1500	1000	647
3	4633	3894	3318	2750	1682	1281	895
4	5000	4000	3488	2944	2000	1483	1000
5	5220	4020	3675	3000	2075	1500	1155
6	5500	4286	3945	3152	2260	1720	1500
7	6000	5000	4000	3461	2465	2000	1549
8	7000	5220	4677	3750	2803	2098	2000
9	7486	5461	5000	4000	3000	2793	2176

Some definitions:

$j := 0..20$

$YS := \frac{YS}{1000}$ $ZS := \frac{ZS}{1000}$ Scale section data to m.

$L := 124.5$ $\rho := 1025$ $g := 9.81$

Input initial draft (to hull keel line) at AP (first) and FP (second):

Ts :=

	0
0	4.950
1	4.990

AP

TA := Ts₀

FP

TF := Ts₁

Function Statements

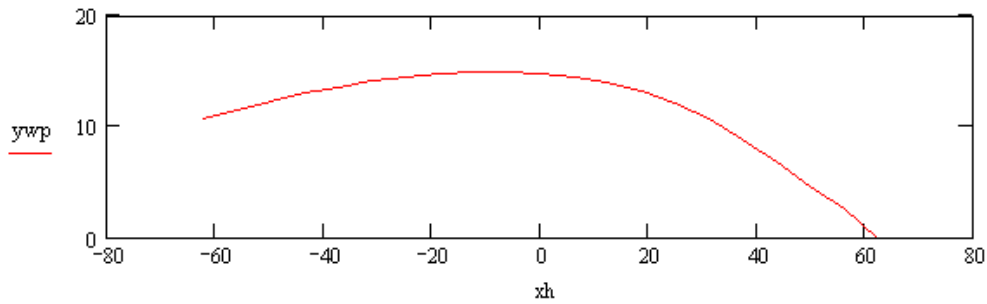
$$T(J, T_a, T_f) := T_a + \frac{J}{20} \cdot (T_f - T_a) \quad \text{Draft}$$

$$Y(Z, J) := \text{linterp}(ZS^{(J)}, YS^{(J)}, Z) \quad Y(Z)$$

$$ywp_j := 2 \cdot Y(T(j, T_a, T_f), j) \quad \text{Waterplane breadth}$$

$$ywp_j := \text{if}(ywp_j > 0, ywp_j, 0) \quad ywp_{20} := 0$$

$$xh_j := \frac{L}{20} \cdot (j - 10) \quad \text{Axial coordinate wrt midships, x fwd}$$



$$Ywp(x) := \text{linterp}(xh, ywp, x)$$

$$A_{WP} := \int_{xh_0}^{xh_{20}} Ywp(x) \, dx \quad A_{WP} = 1437.7788 \quad \text{Waterplane area}$$

$$TPI := A_{WP} \cdot \rho \cdot g \quad TPI = 1.4457 \times 10^7 \quad \text{TPI in newtons per metre}$$

$$LCF := \frac{\int_{xh_0}^{xh_{20}} x \cdot Ywp(x) \, dx}{A_{WP}} \quad LCF = -8.0372 \quad \text{wrt midships (negative - aft)}$$

$$I_L := \int_{xh_0}^{xh_{20}} (x - LCF)^2 \cdot Ywp(x) \, dx \quad I_L = 1.3483 \times 10^6$$

$$MCT_d := \frac{I_L \cdot \rho \cdot g \cdot \pi}{180} \quad MCT_d = 2.3662 \times 10^8 \quad \text{MCT in Newton-m per degree}$$

$$MCT_m := \frac{I_L \cdot \rho \cdot g}{L} \quad MCT_m = 1.0889 \times 10^8 \quad \text{MCT in Newton-m per metre}$$

Input normal (down) force and pitching moment about midships

zm :=

	0	
0	$3.58 \cdot 10^6$	Z
1	$-1.57 \cdot 10^7$	M

Shift moment to LCF:

$$Z := zm_0 \quad Z = 3.5800 \times 10^6$$

$$M := zm_1 \quad M = -1.5682 \times 10^7$$

$$M_{LCF} := M + Z \cdot LCF \quad M_{LCF} = -4.4455 \times 10^7$$

Linear estimates of...

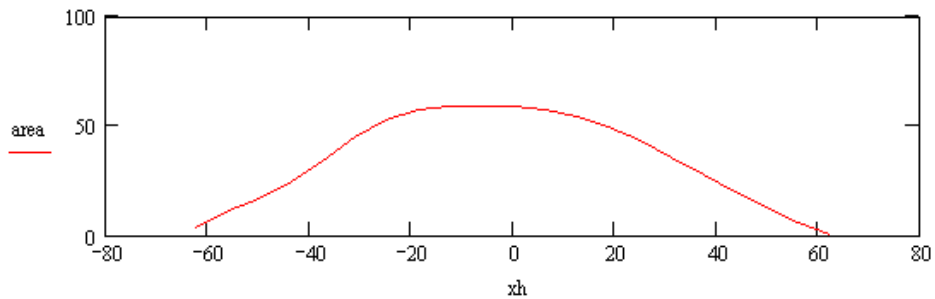
Sinkage: $\Delta z := \frac{Z}{TPI} \quad \Delta z = 0.24763 \quad \text{metres, at LCF}$

Trim: $\Delta \theta := \frac{M_{LCF}}{MCT_d} \quad \Delta \theta = -0.18788 \quad \text{degrees}$

$\frac{M_{LCF}}{MCT_m} = -0.40825 \quad \text{metres, positive by stern}$

Volumetric Properties:

$$area_j := \text{if} \left(ZS_{0,j} < T(j, TA, TF), 2 \cdot \int_{ZS_{0,j}}^{T(j, TA, TF)} Y(z, j) dz, 0 \right)$$



$Area(x) := \text{linterp}(xh, area, x)$

(Note, trapezoidal integration will underestimate volumetric properties by a little bit.)

$$Vol := \int_{xh_0}^{xh_{20}} Area(x) dx \quad \frac{Vol \cdot \rho}{1000} = 4630.6155 \quad \text{Salt water displacement, t.}$$

$$Z_{\text{init}} := \rho \cdot g \cdot \text{Vol} \qquad Z_{\text{init}} = 4.5426 \times 10^7 \qquad \text{Initial Z (hydrostatic force)}$$

$$\text{MomV} := \int_{xh_0}^{xh_{20}} x \cdot \text{Area}(x) \, dx$$

$$M_{\text{init}} := \rho \cdot g \cdot \text{MomV} \qquad M_{\text{init}} = -1.0861 \times 10^8 \qquad \text{Initial M (hydrostatic moment)}$$

$$\text{LCB} := \frac{\text{MomV}}{\text{Vol}} \qquad \text{LCB} = -2.3910 \qquad \text{(relative to midships)}$$

Iterated Estimates:

Definitions: $Z_T := Z_{\text{init}} + Z$ Initial + Squat Force and moment Note: $\frac{Z}{Z_{\text{init}}} = 0.0788$

$M_T := M_{\text{init}} + M$ $\frac{M}{M_{\text{init}}} = 0.1444$

$$TA_n(dz, d\theta) := TA + dz + \left(\text{LCF} + \frac{L}{2} \right) \cdot \tan\left(d\theta \cdot \frac{\pi}{180} \right)$$

$$TF_n(dz, d\theta) := TF + dz + \left(\text{LCF} - \frac{L}{2} \right) \cdot \tan\left(d\theta \cdot \frac{\pi}{180} \right)$$

At AP: $TA_n(\Delta z, \Delta \theta) - TA = 0.0699 \text{ m}$ (Linear squat)

At FP: $TF_n(\Delta z, \Delta \theta) - TF = 0.4781 \text{ m}$

$$T_n(J, dz, d\theta) := TA_n(dz, d\theta) + \frac{J}{20} \cdot (TF_n(dz, d\theta) - TA_n(dz, d\theta))$$

$$\text{area}_n(J, dz, d\theta) := \text{if} \left(ZS_{0,J} < T_n(J, dz, d\theta), 2 \cdot \int_{ZS_{0,J}}^{T_n(J, dz, d\theta)} Y(\zeta, J) \, d\zeta, 0 \right)$$

$$\text{Area}_n(x, dz, d\theta) := \begin{cases} \text{for } k \in 0..20 \\ A_k \leftarrow \text{area}_n(k, dz, d\theta) \\ \text{linterp}(xh, A, x) \end{cases}$$

$$\delta z := \Delta z \qquad \delta \theta := \Delta \theta$$

Solve Loop

Given

$$Z_T = \rho \cdot g \int_{x_{h_0}}^{x_{h_{20}}} \text{Area}_n(x, \delta z, \delta \theta) dx$$

$$M_T = \rho \cdot g \int_{x_{h_0}}^{x_{h_{20}}} x \cdot \text{Area}_n(x, \delta z, \delta \theta) dx$$

$$\begin{pmatrix} \Delta z \\ \Delta \theta \end{pmatrix} := \text{Find}(\delta z, \delta \theta) \quad (\text{may be disabled})$$

$$\Delta z = 0.2457 \quad \text{m (at LCF)}$$

$$\Delta \theta = -0.0530 \quad \text{degrees}$$

Iterated Squat

$$\text{At AP:} \quad T_{A_n}(\Delta z, \Delta \theta) - T_A = 0.1955 \quad \text{m}$$

$$\text{At FP:} \quad T_{F_n}(\Delta z, \Delta \theta) - T_F = 0.3108 \quad \text{m}$$

Annex B. Hydrostatic Calculation Worksheet for Submarine

With minor modifications, the procedure shown on the next four pages could be used for any surfaced submarine or vehicle for which the hull is axisymmetrical.

Longitudinal coordinate x , positive aft, and hull diameter are entered into the input tables `hp` for arbitrary stations, starting at the FP. Right-click within each table and select “Import” to read an ASCII file of values; a modified PC967A input file was used in this instance. Normal force and pitching moment from PC967, which are entered near the top of the third page of the worksheet, must be in standard submarine coordinates (Z downwards, M bow up).

Linear squat estimates are made as in annex A. For the iterated estimates, section area is an analytical function of local sinkage. The right-hand sides of equations (4) and (5) are therefore single integrals, and solving for Δz and $\Delta\theta$ is much faster than for the worksheet in annex A.

AXHULL_STAT_2.MCD

Input Table for x and diameter, x going aft (can use modified PC967A.INP file.):

hp :=

	0	1
0	-74.9	0
1	-71.35	7.3
2	-67.6	8.9
3	-63.85	10.2
4	-60.1	11.4
5	-56.35	12.5

(right-click a cell and
"import" to change file)

$$N := \text{length}(hp^{(0)}) - 1$$

$$n := 0..N$$

$$N = 40.0000$$

$$xh_n := -hp_{N-n,0}$$

Assign columns; sort
(N fwd, 0 aft); set x fwd

$$dia_n := hp_{N-n,1}$$

$$D := \max(dia) \quad D = 12.8000$$

$$L := xh_N - xh_0$$

$$L = 149.8000$$

Input Table for initial draft (to hull keel line) at AP (first) and FP (second):

Ts :=

	0
0	9.915
1	8.085

AP

$$TA := Ts_0$$

FP

$$TF := Ts_1$$

$$Q := \frac{TA - TF}{L}$$

$$d_n := TA - Q \cdot (xh_n - xh_0) - \frac{D}{2}$$

depth of hull axis

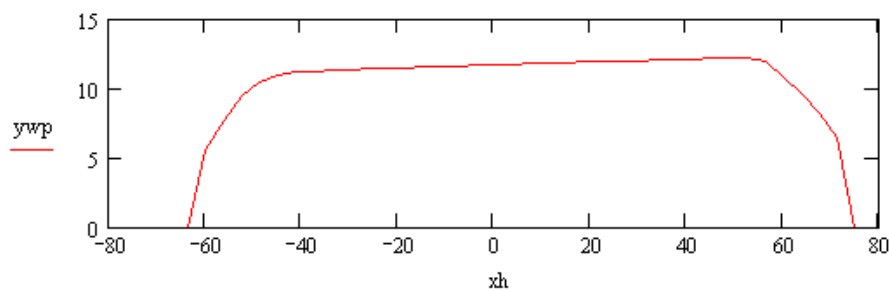
$$disc_n := \frac{(dia_n)^2}{4} - (d_n)^2$$

$$ywp_n := \text{if}(disc_n > 0, 2 \cdot \sqrt{disc_n}, 0)$$

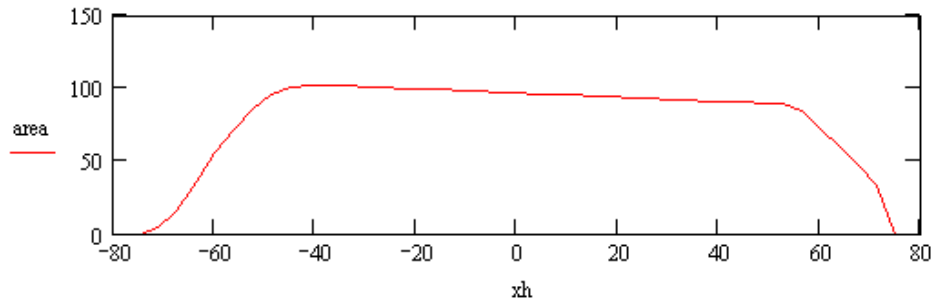
width of waterplane

$$f_n := \text{if}\left(dia_n > 0, \frac{2 \cdot d_n}{dia_n}, 1\right)$$

(above, "1" is arbitrary)



$$area_n := \text{if}\left[disc_n > 0, \frac{(dia_n)^2}{4} \left[\pi - \left(\arccos(f_n) - \frac{ywp_n}{dia_n} \cdot f_n \right) \right], \frac{(dia_n)^2}{4} \cdot \pi \right]$$



$$\rho := 1025 \quad g := 9.81$$

$$\text{Area}(x) := \text{linterp}(xh, \text{area}, x) \quad (\text{i.e., trapezoidal integration})$$

$$\text{Vol} := \int_{xh_0}^{xh_N} \text{Area}(x) \, dx \quad \text{Vol} = 1.2184 \times 10^4$$

$$Z_{\text{init}} := \rho \cdot g \cdot \text{Vol} \quad Z_{\text{init}} = 1.2252 \times 10^8$$

$$\text{MomV} := \int_{xh_0}^{xh_N} x \text{Area}(x) \, dx \quad M_{\text{init}} := \rho \cdot g \cdot \text{MomV} \quad M_{\text{init}} = 1.8985 \times 10^8$$

$$\text{LCB} := \frac{\text{MomV}}{\text{Vol}} \quad \text{LCB} = 1.5496$$

These are relative to midships.

Initial Estimates:

$$Y_{wp}(x) := \text{linterp}(xh, y_{wp}, x) \quad (\text{implies trapezoidal integration})$$

$$A_{WP} := \int_{xh_0}^{xh_N} Y_{wp}(x) \, dx \quad A_{WP} = 1483.6074$$

$$\text{TPI} := A_{WP} \cdot 1025 \cdot 9.81 \quad \text{TPI} = 1.4918 \times 10^7 \quad \text{TPI in Newtons per metre}$$

$$\text{LCF} := \frac{\int_{xh_0}^{xh_N} x Y_{wp}(x) \, dx}{A_{WP}} \quad \text{LCF} = 6.6629 \quad \text{relative to midships.}$$

$$I_L := \int_{xh_0}^{xh_N} (x - \text{LCF})^2 Y_{wp}(x) \, dx \quad I_L = 2.0173 \times 10^6$$

$$MCT_d := \frac{I_L \cdot \rho \cdot g \cdot \pi}{180} \quad MCT_d = 3.5403 \times 10^8 \quad \text{MCT in Newton-m per degree}$$

$$MCT_m := \frac{I_L \cdot \rho \cdot g}{xh_N - xh_0} \quad MCT_m = 1.3541 \times 10^8 \quad \text{MCT in Newton-m per metre}$$

Input Table for normal (down) force and pitching moment about midships
(since that is where PC967 calculates it).

zm :=	
	0
0	7.841·10 ⁵
1	-1.3714·10 ⁷

$$Z := zm_0 \quad Z = 7.8410 \times 10^5$$

$$M := zm_1 \quad M = -1.3714 \times 10^7$$

$$M_{LCF} := M + Z \cdot LCF \quad M_{LCF} = -8.4897 \times 10^6$$

Estimated Sinkage and Trim:

wrt LCF: $\Delta z := \frac{Z}{TPI} \quad \Delta z = 0.05256 \quad \text{metres}$

(since MCT is based on that) $\Delta \theta := \frac{M_{LCF}}{MCT_d} \quad \Delta \theta = -0.02398 \quad \text{degrees}$

(Trim, FP to AP in m) $\frac{M_{LCF}}{MCT_m} = -0.06270 \quad \text{metres, positive by stern}$

Iterated Estimates...

Definitions: $Z_T := Z_{init} + Z \quad Z_T = 1.2330 \times 10^8$
 $M_T := M_{init} + M \quad M_T = 1.7614 \times 10^8 \quad \text{Relative to midships}$

$$TA_n(dz, d\theta) := TA + dz + (LCF - xh_0) \cdot \tan\left(d\theta \cdot \frac{\pi}{180}\right) \quad \text{dz is taken at LCF; also assume small angle, etc. ...}$$

$$d_n(X, dz, d\theta) := TA_n(dz, d\theta) - (X - xh_0) \cdot \left(Q + \tan\left(d\theta \cdot \frac{\pi}{180}\right)\right) - \frac{D}{2}$$

$$disc_n(X, DA, dz, d\theta) := \frac{DA^2}{4} - d_n(X, dz, d\theta)^2$$

$$ywp_n(X, DA, dz, d\theta) := \text{if}(\text{disc}_n(X, DA, dz, d\theta) > 0, 2 \cdot \sqrt{\text{disc}_n(X, DA, dz, d\theta)}, 0)$$

$$f_n(X, DA, dz, d\theta) := \text{if}\left(DA > 0, \frac{2 \cdot d_n(X, dz, d\theta)}{DA}, 1\right)$$

$$g_n(X, DA, dz, d\theta) := \frac{DA^2}{4} \cdot \left[\pi - \left(\text{acos}(f_n(X, DA, dz, d\theta)) - \frac{ywp_n(X, DA, dz, d\theta)}{DA} \cdot f_n(X, DA, dz, d\theta) \right) \right]$$

$$\text{area}_n(X, DA, dz, d\theta) := \text{if}\left(\text{disc}_n(X, DA, dz, d\theta) > 0, 1 \cdot g_n(X, DA, dz, d\theta), \frac{DA^2}{4} \cdot \pi\right)$$

$$\text{Dia}(X) := \text{linterp}(xh, dia, X) \quad \text{and} \quad \delta z := \Delta z \quad \delta \theta := \Delta \theta$$

Solve Loop: Given

$$Z_T = \rho \cdot g \int_{xh_0}^{xh_N} \text{area}_n(x, \text{Dia}(x), \delta z, \delta \theta) dx$$

$$M_T = \rho \cdot g \int_{xh_0}^{xh_N} x \cdot \text{area}_n(x, \text{Dia}(x), \delta z, \delta \theta) dx$$

$$\begin{pmatrix} \Delta z \\ \Delta \theta \end{pmatrix} := \text{Find}(\delta z, \delta \theta) \quad (\text{may be toggled off})$$

Which gives the iterated estimates.....

Estimated Sinkage: $\Delta z = 0.07015$ metres (at LCF)

Estimated Trim: $\Delta \theta = 0.03916$ degrees

(These values are for default tolerances less one OOM; results using the default tolerances are essentially the same for these test data.)

Resulting draft at AP and FP:

$$\text{AP} \quad TA_n(\Delta z, \Delta \theta) = 10.04089 \quad \text{m}$$

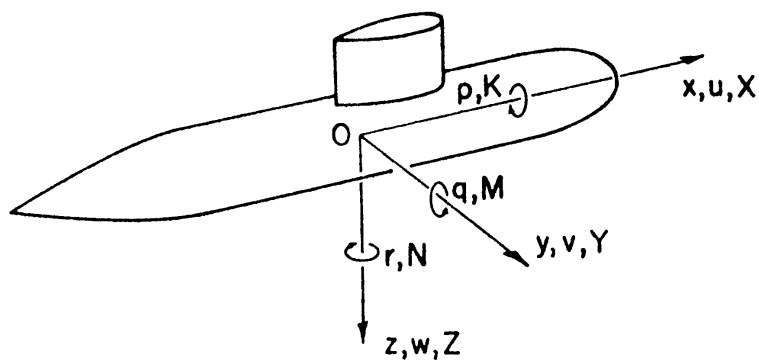
$$\text{FP} \quad TA_n(\Delta z, \Delta \theta) - L \cdot \left(Q + \tan\left(\Delta \theta \cdot \frac{\pi}{180}\right) \right) = 8.10851 \quad \text{m}$$

Nomenclature

Symbols

a	radius of a sphere
A_{WP}	waterplane area
$B(x), B$	beam, maximum beam
c	bottom clearance
C_B	nondimensional LCB
C_F	nondimensional LCF
c_P	pressure coefficient
C_P	prismatic coefficient
C_W	waterplane coefficient
c_Z	nondimensional downforce based on πa^2 or πr^2
c_z	Vermeer's sinkage coefficient, equation (13)
c_θ	Vermeer's trim coefficient, equation (14)
F_h	Froude number based on depth
F_r	Froude number based on hull length
g	gravitational acceleration
h	depth or height above bottom
I_L	waterplane moment of inertia
k_W	waterplane longitudinal radius of gyration
K, M, N	roll, pitch, and yaw moment
L	hull length
r	maximum hull radius
s	squat
$S(x), S$	immersed area, maximum area
T	draft
U	forward speed
x, y, z	vehicle body axes
X, Y, Z	axial, lateral, and normal force
δ^*	boundary layer displacement thickness
∇	immersed volume
ρ	density
ϕ, θ, ψ	roll, pitch, and yaw angles
Φ	flow potential

Axes and Loads



Acronyms, Abbreviations, and Subscripts

AP	Aft Perpendicular
BOW	(subscript) forward, generally FP
CF	Canadian Forces
DRDC	Defence R&D Canada
FP	Forward Perpendicular
MID	(subscript) midships
LCF	longitudinal center of floatation
LCB	longitudinal center of buoyancy

Unclassified

DOCUMENT CONTROL DATA		
1. ORIGINATOR Defence R&D Canada – Atlantic	2. SECURITY CLASSIFICATION Unclassified	
3. TITLE Estimation of Submarine Near-Bottom Hydrodynamic Loads and Squat		
4. AUTHORS M. Mackay		
5. DATE OF PUBLICATION April 2003	6a. NO. OF PAGES 47	6b. NO. OF REFS 19
7. DESCRIPTIVE NOTES DRDC Atlantic Technical Memorandum		
8. SPONSORING ACTIVITY		
9a. PROJECT OR GRANT NO. 11GL12	9b. CONTRACT NO.	
10a. ORIGINATOR'S DOCUMENT NUMBER DRDC Atlantic TM 2003–078	10b. OTHER DOCUMENT NOS.	
11. DOCUMENT AVAILABILITY Unlimited		
12. DOCUMENT ANNOUNCEMENT (if different from 11)		
13. ABSTRACT <p>This memorandum outlines a method for estimating the near-bottom loads on a submarine submerged in deep water and for the related problem of predicting submarine squat in deep or shallow water. The method is fully three-dimensional, but has some limitations associated with potential flow and linearization of the free surface. The chief difficulty for this study was the dearth of suitable data available for validation. Nevertheless, the results are encouraging. Overall, it appears that the sinkage component of squat is predicted with greater accuracy than is trim. Further work should include the acquisition of more, reliable, model data and the investigation of scale effects.</p>		
14. KEYWORDS Submarine Hydrodynamics Near-bottom Squat		

Defence R&D Canada

**Canada's leader in defence
and national security R&D**

R & D pour la défense Canada

**Chef de file au Canada en R & D
pour la défense et la sécurité nationale**



www.drdc-rddc.gc.ca